JPET Fast Forward. Published on July 27, 2018 as DOI: 10.1124/jpet.118.249375
This article has not been copyedited and formatted. The final version may differ from this version.

Amelioration of Diabetic Nephropathy Using a Retinoic Acid Receptor β2 Agonist

Steven E. Trasino, Xiao-Han Tang, Maria M. Shevchuk, Mary E. Choi, and Lorraine J. Gudas

1. Department of Pharmacology, Weill Cornell Medical College of Cornell University, New York, NY (SET, XT, LJG)
2. School of Urban Public Health, Nutrition Program, Hunter College, City University of New York, New York, NY (SET)
3. Department of Pathology, Weill Cornell Medical College of Cornell University, New York, NY (MMS)
4. Division of Nephrology and Hypertension, Department of Medicine, Weill Cornell Medical College of Cornell University, New York, NY (MEC)
5. New York-Presbyterian Hospital-Weill Cornell Medical Center, New York, NY (MEC)

Running Title: Retinoic Acid Receptor β2 Diminishes Diabetic Nephropathy

Corresponding author: Lorraine J. Gudas, Ph.D., Department of Pharmacology, Weill Cornell Medical College, 1300 York Avenue, New York, NY, 10065; telephone: 212-746-6250; email: ljgudas@med.cornell.edu

Text Pages: 45

Tables: 1 Supplemental Table

Figures: 7 Figures and 3 Supplemental Figures

References: 99

Word Count:

Abstract: 246

Introduction: 846 (including references)

Discussion: 1,717 (including references)

Abbreviations: AC261: AC261066, a retinoic acid receptor β2 selective agonist; ACR: albumin to creatinine ratio; Aldh1a2: aldehyde dehydrogenase, member 1a2; α-SMA: α-smooth muscle actin; AUC: area under the curve; CKD: chronic kidney disease; Col-IV: collagen IV; Crbp1: cellular retinol binding protein 1; Cyp26a1: cytochrome P-450, member 26 a1; DN: diabetic nephropathy; ECs: endothelial cells; GBM: glomerular basement membrane; GFB: glomerular filtration barrier; H&E: hematoxylin and eosin; HFD: high fat diet; IHC: immunohistochemistry; IPGTT: intraperitoneal glucose tolerance test; LDs: lipid droplets; MWS: Matthew-Wood syndrome; PAS: periodic acid-schiff; PODs: podocytes; q-PCR: quantitative PCR; RA: retinoic acid; RAR: retinoic acid receptor; RBP4: retinol binding protein-4; RC: renal cancer; ROL: retinol, SEM: standard error of the mean; STRA6: stimulated by retinoic acid 6; TECS: tubule epithelial cells; TEM: transmission electron microscopy; T2D: type 2 diabetes; VA: vitamin A; VAD: vitamin A deficient; WT1: Wilms' tumor-suppressor gene 1.

Section Assignment: Gastrointestinal, Hepatic, Pulmonary, and Renal

ABSTRACT.

Vitamin A (VA) and its derivatives, known as retinoids, play critical roles in renal development through retinoic acid receptor β2 (RARβ2). Disruptions in VA signaling pathways are associated with the onset of diabetic nephropathy (DN). Despite the known role of RARβ2 in renal development, the effects of selective agonists for RARβ2 in a high fat diet (HFD) model of DN are unknown. Here we examined whether AC261066 (AC261), a highly selective agonist for RARβ2, exhibited therapeutic effects in a HFD model of DN in C57BL/6 mice. Twelve weeks of AC261 administration to HFD-fed mice was well-tolerated, with no observable side effects. Compared to HFD-fed mice, HFD+AC261 treated mice had improved glycemic control and reductions in proteinuria and urine albumin to creatinine ratio (ACR). A number of cellular hallmarks of DN were mitigated in HFD+AC261 treated mice, including reductions in tubule lipid droplets (LDs), podocyte (POD) effacement, endothelial cell (EC) collapse, mesangial expansion, and glomerular basement membrane (GBM) thickening. Mesangial and tubule interstitial expression of the myofibroblast markers α-smooth muscle actin (α-SMA) and type IV collagen (Col-IV) was lower in HFD+AC261 treated mice compared to HFD alone. Ultrastructural and immunohistochemistry (IHC) analyses showed that, compared to HFD-fed mice, HFD+AC261 treated mice showed preservation of POD foot process and slit diaphragm morphology, an increase in the levels of slit-diagram protein podocin and the transcription factor WT1 in PODs. Given the need for novel DN therapies, our results warrant further studies of the therapeutic properties of AC261 in DN.

INTRODUCTION.

Diabetic nephropathy (DN) is the most common cause of end-stage renal disease (de Boer et al., 2011), and is the single strongest predictor of mortality from cardiovascular disease in patients with type 2 diabetes (T2D) (Stratton et al., 2000; Valmadrid et al., 2000). Clinically, DN is characterized by the onset of glomerular lesions, progressive loss of glomerular filtration rate, albuminuria, and hypertension (Tervaert et al., 2010). Intervention trials have demonstrated that intensive glycemic and hypertension control for DN has limited therapeutic effectiveness (Parving et al., 2012; Fried et al., 2013; Gentile et al., 2014; Hajhosseiny et al., 2014). Thus, given the limitations of current DN therapies, there is an urgent need to identify molecules that can therapeutically modulate relevant kidney cell types and pathways central to the pathogenesis of DN (Gentile et al., 2014).

Vitamin A (VA, retinol) is an essential micronutrient that, primarily acting through its biologically active metabolite all-*trans*-retinoic acid (RA) and RA receptors (RAR α, β and γ), regulates the expression of genes that are vital to reproduction, organogenesis, and adult human health (Chambon, 1996; Gudas, 2012). Normal kidney development is highly dependent on RA signaling (Gilbert, 2002), as the severe renal malformations and reduced numbers of nephrons that occur in VA deficient (VAD) newborn mice can be reversed with exogenous RA (Lelièvre-Pégorier et al., 1998). In developing kidney rudiments RA is synthesized locally (Rosselot et al., 2010; Gudas, 2012), and acting through RARα and RARβ2, modulates the expression of the receptor tyrosine kinase and c-ret (Ret) (Batourina et al., 2001; Batourina et al., 2002; Rosselot et al., 2010), which direct nephron differentiation and branching of the ureteric bud (Batourina et al.,

2001). Through a highly conserved retinoic acid responsive element, RA-RARβ2 also regulates expression of Wilms' tumor-suppressor gene 1 (WT1) (Bollig et al., 2009), a master transcriptional regulator of glomerular cell development (Kreidberg et al., 1993; Palmer et al., 2001). Mice that lack RARβ2 or RARα exhibit severe renal malformations, and reduced kidney mass and nephron numbers (Mendelsohn et al., 1999).

In the adult kidney, cells in the glomerulus and tubule epithelial cells (TEC) are responsible for VA-retinol binding protein-4 (RBP4) recycling (Blomhoff et al., 1990; Raila et al., 2005), and as such, perturbations in VA-RBP4 homeostasis have been observed in DN (Smith and Goodman, 1971; Raila et al., 2007; Frey et al., 2008). Despite the well-established role of the kidney in maintenance of whole body VA homeostasis (Blomhoff et al., 1990; Raila et al., 2005), the molecular actions of VA, RA, and the RARs on renal parenchymal cell functions are still emerging. However, a convincing body of data demonstrates that VA, acting through RA, shows protective properties in several renal diseases (Lazzeri et al., 2014; Mallipattu and He, 2015), such as experimental glomerulonephritis (Wagner et al., 2000; Schaier et al., 2001; Lehrke et al., 2002; Perez et al., 2004; Chiba et al., 2016), HIV-associated nephropathy (Lu et al., 2008; Ratnam et al., 2011), and DN (Han et al., 2004; Kim et al., 2015).

RA favorably modulates the functions of several cell types vital to the glomerular filtration barrier (Anderson et al., 1998; Vaughan et al., 2005; Su et al., 2012; Zhang et al., 2012). Perturbations in renal VA metabolism and RA signaling appear to be involved in the onset of DN, as reductions in renal VA metabolism and RA signaling occur in mouse and human T2D-DN (Raila et al., 2007; Frey et al., 2008; Starkey et al., 2010; Trasino et al., 2015; Jing et al., 2016) and albuminuria promotes progression of renal

injury by inhibiting RA-mediated differentiation of podocyte progenitors (Peired et al., 2013). Pharmacological approaches that increase podocyte responsiveness to RA signaling mitigate progression of experimental renal injury (Sagrinati et al., 2006; Lasagni et al., 2015). However, given the aberrant renal metabolism of VA and RA in T2D and DN (Trasino et al., 2015), a novel approach for development of retinoid-mediated DN therapies is the use of synthetic agonists for RARs, as they not as likely to be affected by altered VA metabolism that occurs in T2D-DN (Starkey et al., 2010; Trasino et al., 2015; Jing et al., 2016). RARβ is expressed predominantly in glomerular cells in the adult kidney (Manzano et al., 2000; Zhong et al., 2011; Uhlén et al., 2015), and RARβ2 is the most relevant RARβ isotype in renal development (Batourina et al., 2001). Thus, we tested the anti-DN properties of an orally available agonist selective for RARβ2 (AC261066) (Lund et al., 2005; Lund et al., 2009), which we previously demonstrated possesses anti-diabetic properties in murine models of obesity and T2D (Trasino et al., 2016b; Trasino et al., 2016a). To date, studies of the renal protective properties of RA or RAR specific agonists have not utilized high fat dietary (HFD) models of DN (Wei et al., 2004; Brosius et al., 2009; Deji et al., 2009); therefore, in light of our previous work demonstrating the anti-T2D properties of AC261066 in HFD-models of T2D (Trasino et al., 2016b; Trasino et al., 2016a), in the current study we examined if AC261066 possesses renal protective properties in a HFD-model of DN.

MATERIALS AND METHODS.

High Fat Dietary Model of Diabetic Nephropathy and Drug Treatments: All animal experiments were conducted in accordance with the Guide for the Care and Use of Laboratory Animals as adopted and promulgated by the U.S. National Institutes of Health and the Institutional Animal Care and Use Committee (IACUC) guidelines at Weill Cornell Medical College (WCMC). A high-fat diet (HFD) fed C57BL/6 mouse model of DN was utilized for this study, as this model results in obesity, insulin resistance, and renal injury; the renal injury exhibits a number of features of human DN, including microalbuminuria, podocytopenia, glomerular hypertrophy, basement membrane thickening, mesangial expansion, and renal lipid accumulation (Brosius et al., 2009; Deji et al., 2009).

Diabetic Nephropathy Model: Wild type (Wt), 10-week old, male C57BL/6 mice fed a standard laboratory chow (13% kcal fat, #5053, Pico Diet, St. Louis, MO) were randomized to either: remain on a laboratory chow (control, n=4), or a high fat, diabetic nephropathy diet (HFD, n=8) (45% kcal fat, #58125, Test Diets, St. Louis, MO) for 16-weeks. Four weeks after beginning HFD treatment, HFD groups were further randomized to: i) remain on the HFD diet, plus drinking water containing 0.2% DMSO (HFD, n=4); or ii) the HFD diet, plus drinking water containing 3.0 mg/100 ml of AC261066 (AC261) [in 0.2% DMSO] (HFD+AC261, n=4), a highly selective, orally bioavailable RARβ2 agonist (Lund et al., 2005), for 12-weeks. At the end of the study, mice from all groups were subjected to intraperitoneal glucose tolerance testing (IPGTT) as previously described (Trasino et al., 2016b), spot urine analysis (Kurien and Scofield, 1999), and then mice were sacrificed for tissue harvesting and analysis.

Renal Histology Analysis from BKS-db/db Mice: Renal tissue samples from 16-week-old male C57Bl/6 BKS-db/db mice Cg-Dock7^{m}+/+ Lepr^{db}/J (BKS-db, Stock # 000642) mice (Jackson Labs, Bar Harbor, ME) were evaluated to determine the effects AC261 on renal histological markers of DN. BKS-db/db mice spontaneously develop severe insulin resistance by 4-5 weeks of age (Hummel et al., 1966), and are frequently used as a DN model because they develop a number of renal histological features of DN, including glomerulosclerosis, podocytepenia and mesangial expansion (Sharma et al., 2003). Fourteen-week-old, male BKS-db/db mice were maintained on standard laboratory chow (Con) with 13% kcal fat (#5053, Pico Diet, St. Louis, MO) and randomized to receive: i) drinking water containing 0.2% DMSO; or ii) drinking water containing 3.0 mg/100 ml of AC261 [in 0.2% DMSO] for 14 days.

Morning Spot Urine Analysis: For determination of albuminuria, morning urine samples were obtained as previously described (Kurien and Scofield, 1999) on a single urine collection from two experimental cohorts of control mice (n=5), HFD-fed mice (n=5) and HFD-fed mice treated with AC261 (n=3) as described above. Urine samples were centrifuged at 10,000 x g for 3 minutes at 4°C to remove cellular debris and stored at -70°C until analysis. Urine samples were analyzed for albumin and creatinine using Mouse Albumin ELISA (Molecular Innovations, Novi, MI) and Mouse Creatinine ELISA kits (BioAssay Systems, Hayward, CA) respectively, according to the manufacturer's instructions. To ensure that differences in urine volumes would not affect the albuminuria analyses we compared creatinine normalization of urine albumin levels with urine specific gravity (osmolality, mOsm) normalized urine albumin levels, and had similar findings.

Immunohistochemistry: Renal tissue samples were fixed and processed for immunohistochemistry (IHC) as previously described (Trasino et al., 2016b). Deparaffinized kidney tissue sections were incubated with the following antibodies overnight at 4°C: Podocin (goat anti-mouse, IgG 1:200; Santa Cruz, sc-22298), Wilms' tumor 1 (WT1) (rabbit anti-mouse, IgG 1:100; Santa Cruz, sc-192), smooth muscle actin-α (α-SMA) (mouse anti-mouse, monoclonal IgG1, 1:500; Dako, clone 1A4) and collagen IV (rabbit anti-mouse, IgG 1:200; Novus Biological, NB120-6586). After incubation with secondary antibodies (Super Picture™ Polymer Detection Kit, Invitrogen), signals were visualized based on a peroxidase detection mechanism with a 3,3-diaminobenzidine (DAB) substrate.

Quantitation of DAB IHC: For quantitation of IHC of renal podocin, WT1, α-SMA, and collagen IV, analysis was performed using 4-5 DAB positive fields per slide, with 3-4 slides per mouse (7 μm between each slide sections), and 3-4 mice per group, for a total of 40-50 DAB-positive fields per experimental group. DAB positive slide fields were photographed using a Nikon TE2000-inverted light microscope and digital images were analyzed for DAB densitometry by color deconvolution using Fiji, ImageJ software as described (Schindelin et al., 2012).

Glomerular Area Studies: We stained paraffin-embedded kidney sections with hematoxylin and eosin (H&E) and Periodic Acid Schiff (PAS) using standard histology protocols for histopathology evaluation (Tervaert et al., 2010). We performed glomerular area studies as described (Krendel et al., 2009). Digital images of H&E, PAS stained kidney sections were analyzed for mean glomerular area and PAS densitometry using Fiji, ImageJ software (Schindelin et al., 2012); 50-60 glomeruli per animal (with 4

animals per experimental group), were used to determine mean glomerular area in the HFD-DN, and BKS-db/db DN mouse cohorts.

Renal Histopathology: Renal sections were separately analyzed by a pathologist and nephrologist in a blinded manner and classified according to DN histopathologic classification (Tervaert et al., 2010). For each kidney sample, 40-50 H&E and PAS stained cross-sections of glomeruli were analyzed and scored using the following scoring system: 0, normal glomerulus; +1, mesangial matrix expansion of the glomerulus; +2, severe mesangial matrix expansion; +3, severe mesangial matrix expansion and/or segmental glomerulosclerosis; and +4, global glomerulosclerosis (>50% of the glomerulus). The mean glomerular score for each mouse was averaged for each treatment group. Interstitial damage was assessed with respect to interstitial fibrosis as described (Sastre et al., 2013).

Transmission Electron Microscopy Analysis of Glomerular Ultra Morphological Lesions: We processed fresh kidney samples for transmission electron microscopy (TEM) as described (Szeto et al., 2017). Freshly isolated renal tissue was fixed in 4% paraformaldehyde followed by post-fixation in 1% osmium tetroxide, dehydration in graded alcohols, and embedding in Epon. Ultrathin sections (200–400 Å) were cut on nickel grids, stained with uranyl acetate and lead citrate, and examined in the Weill Cornell Microscopy Core using a digital transmission electron microscope (JEM-1400; JEOL, Ltd., Akishima, Japan).

We evaluated renal TEM sections for the following ultra-morphological changes: 1) diffuse glomerular basement membrane (GBM) thickening, 2) mesangial expansion, 3) podocytopenia, 4) diffuse foot process effacement, 5) electron-dense areas of

hyalinosis in sclerotic nodules, 6) cellular lipid droplets (LDs), and 7) diabetic fibrillosis. We performed quantitative analysis of GBM thickening using the orthogonal intercept method of Jensen (Jensen et al., 1979). Briefly, 10 digital images were captured per animal (5 capillary loops per glomerulus, 5 glomeruli per animal). A grid mask with intercepts was applied to each image and GBM thickness was measured in pixels at each intercept from the basal endothelial to the basal podocyte plasma membranes and converted to nanometers using the image processing software, iTEM (Olympus-SiS, Münster, Germany). Quantitative analysis of mesangial expansion (volume density of mesangium and mesangial matrix) was conducted as described in Guo *et al.* (Guo et al., 2005), podocyte number as in (Weibel ER and DM., 1962), and diffuse foot process effacement according to Deegens *et al.* (Deegens et al., 2008). We evaluated and quantitated ultra-morphological changes to renal TEM sections in a blinded manner as described (Weibel ER and DM., 1962; Jensen et al., 1979; Guo et al., 2005; Deegens et al., 2008).

RNA Isolation and Quantitative RT-PCR: We extracted total RNA from renal cortex tissue preserved in RNA later (Thermo Scientific, Inc.) using the TRIzol reagent (Thermo Scientific, Inc.) from 6-8-week old, wt, male C57BL/6 mice fed either a standard laboratory chow (control, 13% kcal fat, #5053, Pico Diet, St. Louis, MO, n=4), a high fat diet (HFD, 45% kcal fat, #58125, Test Diets, St. Louis, MO, n=4) for ~14 weeks, or a HFD diet for 9 weeks, followed by a HFD but with drinking water containing 3.0 mg/100 ml of AC261066 (AC261) [in 0.2% DMSO] (HFD+AC261, n=4) for 5 weeks. Total RNA (1 µg) was used to synthesize cDNA using the Revert Aid First Strand cDNA Synthesis Kit (Thermo Scientific, Inc.). We performed Quantitative RT-PCR (q-PCR) as

previously described (Trasino et al., 2016b) using SYBR Green PCR master mix on an Agilent Mx3000P Real Time PCR system (Agilent, Inc.). We used gene specific primers (Supplemental Table 1) to amplify mRNAs that were then normalized to the internal control gene, hypoxanthine phosphoribosyltransferase (*Hprt)*. cDNA from four mice (n=4) per experimental group was analyzed for relative mRNA fold changes. We calculated relative gene expression fold changes using the delta, delta Ct method (Livak and Schmittgen, 2001).

High Performance Liquid Chromatography of Renal and Serum Vitamin A (Retinol): Retinol (ROL) was extracted from renal and serum samples using acetonitrile: butanol (50:50, v/v), 0.1% butylated hydroxytoluene and saturated K_2HPO_4 and analyzed by high performance liquid chromatography (HPLC) as previously described (Trasino et al., 2015). ROL was identified in tissue samples based an exact match of the retention times of peaks of pure ROL standards and its UV absorption spectrum. The concentration of the ROL standard was used to calculate ROL concentrations normalized to mg of wet renal tissue weight or volume for serum.

Statistics: All data means were tested and passed normality testing using Shapiro-Wilk normality test (GraphPad Software, Inc.). Group means for data in Figure 1E-F (spot urine analysis and ACR), Figure 3A-D, (IHC for α-SMA and collagen IV) were computed using ANOVA and Bonferroni's multiple comparison test, with group means treated as independent variables due to having less than n=4 per experimental group. Means testing from all other figures were analyzed using repeated measures ANOVA and Bonferroni's multiple comparison test. Group means for all figures are reported as mean ± standard deviation (SD). The number of mice used for each analysis is indicated in

the relevant methods sections and figure legends. Significant differences were defined as p-values with an alpha less than 0.05, and all usage of the term “significant” throughout the text refers to means differences with a $p < 0.05$. All statistical analyses were performed using GraphPad Prism 7.0 statistical software (GraphPad Software, Inc.).

RESULTS.

Treatment with an RARβ2 Agonist Improves Renal Injury and Urine Albumin Excretion in HFD-Fed Mice. Sixteen weeks of HFD feeding led to a 50% increase in body weights (BW) (Figure 1A), and resulted in impaired glucose tolerance compared to chow-fed (control) mice (Figure 1B-D). Treatment with AC261 had no effect on BW (Figure 1A), but, as previously reported, partially restored euglycemia in the HFD+AC261 mice (Figure 1B-D) (Trasino et al., 2016b).

Sixteen weeks of HFD feeding resulted in a ~522% increase in urine albumin excretion and a ~187% increase in urine albumin to creatinine ratio (ACR) (Figure 1E,F). HFD+AC261 treated mice showed 50% and ~40% lower levels of urine albumin and ACR, respectively, compared to HFD alone (Figure 1E,F). As previously reported, AC261 treatment did not affect water or food intake (not shown) (Trasino et al., 2016b).

RARβ2 Agonist Treatment Results in Less Tubule Vacuolization and Glomerular Hypertrophy. The patterns of renal lipid accumulation in the HFD-fed cohort (Figure 2A [b, yellow arrows]); are in agreement with those observed in human DN (Bobulescu et al., 2014; Herman-Edelstein et al., 2014) and murine diet-induced models of T2D (Bobulescu, 2010), with the appearance of tubule epithelial cell (TEC) vacuolization, a marker of cytosolic lipid droplets (LD) and impaired TEC lipid metabolism (Tervaert et al., 2010; Kang et al., 2015). We detected a 2.5-3.0 degree higher TEC vacuolization in HFD-fed mice compared to controls (Figure 2A, [b vs. a, yellow arrows]; 2B, $^{**}p<0.01$), and a significant reduction in tubule vacuolization in HFD+AC261 treated mice, compared to HFD-fed mice (Figure 2A [c vs. b, yellow arrows]; 2B, $^{*}p<0.05$). Consistent with the renal pathology in early human DN (Alsaad and Herzenberg, 2007), Periodic

Acid-Schiff (PAS) and H&E-stained renal sections of HFD-fed mice, compared to controls, showed mild, diffuse expansion of glomerular mesangial matrix (Figure 2C [PAS, b vs. a], 2D ~2.0-fold, ***p<0.001) extending into capillary loop membranes (Figure 2C [PAS, b vs. a, yellow arrows]). HFD-fed mice had marked glomerular hypertrophy (Figure 2C [H&E, d vs. e]), and a significantly increased mean glomerular area compared to controls (Figure 2E, ***p<0.001). Compared to HFD-fed mice, HFD+AC261 treated mice showed less accumulation of PAS-positive material in the mesangium (Figure 2C [PAS, c vs. b]; 2D, **p<0.01) and in capillary loop membranes (Figure 2C [PAS, c vs. b, yellow arrows]); consistent with this, there was less glomerular hypertrophy and a lower mean glomerular area (Figure 2C [H&E, f vs. e]; 2E, *p<0.05).

Lower Expression of α-Smooth Muscle Actin and Collagen IV with the RARβ2 Agonist Treatment. Mesangial cells secrete extracellular matrix proteins, including type IV collagen, laminins, and fibronectin, and various proteoglycans, which provide the functional and structural integrity of the glomerular tuft, including its capillary network (Couchman et al., 1994). In DN and chronic kidney disease, in response to injury glomerular and interstitial mesangial cells dedifferentiate to “mesangiocytes” and synthesize α-SMA and other contractile proteins that contribute to glomerulosclerosis and DN progression (Cook, 2010). Our previous studies have demonstrated that AC261 treatments can reduce liver myofibroblast activation and expression of α-SMA in a murine HFD-model of nonalcoholic fatty liver disease (Trasino et al., 2016a). Therefore, we determined the effects of AC261 on renal α-SMA protein expression by IHC.

In kidneys from control mice, TEC interstitial and glomerular α-SMA protein staining was very weak (Figure 3A [a, red arrow-inset]), but, as expected, staining was

prominent around arterioles (Figure 3A [a, black arrow-inset]). In contrast, in HFD-fed mice, compared to controls, we detected α-SMA protein within glomeruli (Figure 3A [b vs. a]; 3B, ***p<0.001) and in the tubule interstitium (Figure 3A [b vs. a, red arrows-inset]). Compared to HFD-fed mice, the interstitial α-SMA protein level in HFD+AC261 mice was lower (Figure 3A [c vs. b, red arrows-inset]), and intra-glomerular α-SMA protein was also lower (Figure 3A [c vs. b]; 3B, ***p<0.001). Despite the increased expression of α-SMA in HFD-fed mice (Figure 3A, b) and consistent with murine models DN (Brosius et al., 2009), our HFD experiments did not result in glomerular or tubulointerstitial fibrosis (not shown).

We also measured the levels of collagen IV protein, a major contributor to glomerular expansion in DN and renal disease (Couchman et al., 1994), and found, consistent with the mesangial expansion (Figure 2D) and the increased glomerular and interstitial α-SMA (Figure 3A, b), that HFD-fed mice exhibited a 0.5-fold increase in renal collagen IV (Figure 3C, ****p<0.0001) compared to control mice, in both glomerular (Figure 3D [b vs. a, black arrows]) and interstitial (Figure 3D [b vs. a, red arrows]) regions. In contrast, collagen IV protein levels in HFD+AC261 treated mice were lower than those in HFD-fed mice (Figure 3D, [c vs. b]; 3C, ****p<0.0001).

RARβ2 Agonist-Treated Mice Exhibit Less Glomerular Basement Membrane Thickening. Thickening of glomerular basement membrane (GBM) is associated with easy stages of DN and strongly correlates with impaired renal function and albuminuria. By transmission electron microscopy (TEM) we next measured the mean GBM thickness in all groups, and we found an approximate 51% increase in GBM thickness in HFD vs. control mice (Figure 4D, [TEM, b vs. a, black cross]; 4E). By PAS stain,

capillary loops in HFD+AC261 mice were visually well-defined, with less diffuse mesangial expansion into the GBM compared to HFD-fed mice (Figure 2C [c vs. b, yellow arrows]). GBM thickening in HFD+AC261 mice was not as pronounced as in HFD-fed mice, and was visually more consistent with what we observed in controls (Figure 2C [PAS, c vs. b and a, yellow arrows]). By TEM ultrastructural analyses we determined that AC261 treatment of HFD-fed mice resulted in approximately 22% less GBM thickening compared to non-drug treated HFD mice (Figure 4D [TEM, c vs. b, black cross]; 4E). Taken together, these data show that the histological changes in TEC vacuolization and glomerular hypertrophy are consistent with the reductions in proteinuria (Figure 1E,F), and thus an anti-DN effect of AC261 in HFD-fed mice.

Transmission Electron Microscopy Renal Ultrastructural Analysis. Analysis of TEM images of renal sections showed that, compared to control mice that exhibited normal glomerular filtration barrier (GFB) morphology [i.e. numerous interdigitating podocyte foot processes (Figure 4A, red arrows), separated by filtration slits (Figure 4A, black asterisks)], HFD-fed mice had clear evidence of podocyte injury marked by podocyte foot process collapse and effacement (Figure 4B vs. 4A, [TEM, red arrows]; 4D [TEM, b, red arrow]), a reduction in foot process density (Figure 4F, ***p<0.001), and a clear decrease in filtration slits across the GFB (Figure 4B, black asterisks). HFD-fed mice exhibited lipid vacuoles in both podocyte foot processes and endothelial cells (ECs) (Figure 4, yellow arrows), prominent EC injury with evidence of detachment and collapse from the basement membrane (Figure 4B, white arrows), and reductions in EC fenestrations in the GFB (Figure 4B vs. 4A, black arrows). By TEM ultrastructural renal evaluation we found that, compared to kidneys of HFD-fed mice, the kidneys of

HFD+AC261 treated mice showed diminished podocyte injury, with less foot process effacement (Figure 4C vs. 4B, red arrows), a 1.0-fold increase in podocyte foot process density (Figure 4F, ***p<0.001), and filtration slits that more closely resembled those in the controls (Figure 4C vs. 4A, black asterisks). By TEM analysis we also showed that, compared to HFD-fed mice, HFD+AC261 treated mice showed diminished EC injury indicated by decreased identification of EC collapse (Figure 4C vs. 4B, white arrows), increased EC fenestrations (Figure 4C vs. 4B, black arrows), and fewer EC lipid vacuoles (Figure 4C vs. 4B, yellow arrows).

RARβ2 Agonist Preserves Podocytes in HFD-fed Mice. Podocytes form a portion of the glomerular filtration barrier (GFB) (Abrahamson, 2012; Nagata, 2016), and podocyte injury and effacement occur in the progression of DN (Nakamura et al., 2000; Nagata, 2016). Given the evidence from our TEM ultrastructural analysis that AC261 mitigated podocyte foot process effacement and increased podocyte density in the GFB of HFD-fed mice (Figure 4B vs. 4C, 4F), we next asked if AC261 treatment affected the expression of podocin, a key protein in the foot process slit diaphragm structure where it is part of a scaffold complex that is essential in maintaining GFB function (Kawachi et al., 2006) and in preventing foot process effacement and loss (Kawachi et al., 2006; Nagata, 2016). Podocin and other slit diaphragm proteins were reduced in animal DN models (Nakamura et al., 2000), human DN (Dronavalli et al., 2008), and other nephropathies (Johnstone and Holzman, 2006). Control mice showed prominent GBM podocin positive areas, with some podocin expression observed in the mesangium membrane outlines (Fig 5A [a, red arrows]; 5B). Consistent with the presence of proteinuria (Figure 1E,F), GBM and mesangial podocin staining was thinner and fainter

in HFD-fed mice (Figure 5A [b, red arrows]; 5B, ****p<0.001). HFD+AC261 treated mice had immunopositive podocin regions in the GBM and mesangium similar to those observed in control mice (Figure 5A [c, red arrows]; 5B, ****p<0.001).

We also measured expression of WT1, a key transcription factor for renal development (Kreidberg et al., 1993) that in the adult kidney is not only detected in mature podocytes(Palmer et al., 2001), but is also expressed in podocyte progenitors as major regulator of podocyte development during renal organogenesis (Kreidberg et al., 1993). We detected WT1 immunopositive nuclei in podocytes of control mice (Figure 5A [d, red arrows]; 5C), and, similar to the observed podocin staining pattern, we observed a smaller proportion of WT1 positive nuclei in HFD-fed mice compared to controls (Figure 5A [e vs. d, red arrows]; 5C, ***p<0.001). In contrast, WT1 protein in HFD+AC261 treated mice was similar to that detected in controls (Figure 5A [f vs. d, red arrows]; 5C), with an increased number of WT1 positive nuclei compared to HFD mice (Figure 5A [f vs. e, red arrows]; 5C, **p<0.001).

RARβ2 Agonist Modulation of Renal and Podocyte-Specific Gene Expression in HFD-fed Mice. We next measured relative mRNA levels of *WT1*, *podocin* and three other podocyte specific genes *nephrin*, *podocalyxin,* and *synaptopodin* in renal cortex tissue from a HFD-DN cohort of mice using gene specific primers (Supplemental Table 1) and q-PCR. We found that, similar to our IHC results, relative renal mRNA levels of *WT1* and *podocin* in HFD-fed mice were reduced compared to control mice (Figure 6A, ***p<0.001; 6B, **p<0.01), but in comparison to HFD-fed mice, HFD+AC261 treated mice had 2.6-fold (*p<0.05) and 2.7-fold higher (*p<0.05) renal mRNA levels of *WT1* and *podocin*, respectively (Figure 6A,B). Transcript levels of two other podocyte-specific

genes, *nephrin* and *podocalyxin,* were unchanged across all treatments groups (Figure 6C,D). However, we did detect a reduction in renal mRNA levels of the WT1-regulated gene and podocyte basement membrane anchorage-associated protein *synaptopodin* in HFD-fed mice compared to control mice (Figure 6E, **p*<0.05), and 2.0-fold higher mRNA levels of *synaptopodin* in HFD+AC261 treated compared to HFD-fed mice (Figure 6E, **p*<0.05).

We next measured renal mRNA levels of key mediators of the renal renin–angiotensin system (RAS), including Renin, and Angiotensin I converting enzymes 1 and 2 (*Ace1* and *Ace2*) in order to examine if the anti-DN effects of AC261 involve any renal hemostatic changes. Increases in renal transcripts of Ace have been reported in cases of human DN (Konoshita et al., 2006); however, consistent with a previously published, rat HFD-model of DN (Tain et al., 2017), we did not detect significant changes in renal mRNA transcript levels of *Ren*, *Ace1,* and *Ace2* in HFD-fed or HFD+AC261 treated, compared to control mice (Figure 6F,G,H).

In the adult kidney, there is some evidence that renal developmental pathways regulated by WT1 and RA may contribute preservation and maintenance of mature podocytes and podocyte progenitors in the healthy kidney and in response to renal injury (Sagrinati et al., 2006; Dong et al., 2015; Lasagni et al., 2015). Therefore, we next measured renal transcript mRNA levels of *BMP7*, *Pax2,* and *MafB,* three direct transcriptional targets of WT1, in podocyte progenitors during renal development (Hartwig et al., 2010), and *Ret,* a retinoid regulated gene critical to nephrogenesis (Batourina et al., 2001), to determine if the anti-DN effect of AC261 involves modulation of WT1 or retinoid mediated podocyte progenitor or renal developmental pathways. Our

q-PCR analysis showed that relative mRNA levels of *BMP7*, *Pax2, MafB,* and *Ret* were unchanged across all experimental groups (Figure 6I,J,K,L). These q-PCR data demonstrate that the anti-DN properties of AC261 do not involve activation of regenerative, or fetal retinoid-mediated developmental pathways.

RARβ2 Agonist Modulation of Renal Vitamin A-Specific Genes in HFD-fed Mice.

To examine changes to retinoid-mediated pathways, we next measured renal transcript levels of retinoid relevant genes, including *RARα, RARβ2, RARγ,* cellular retinoid binding protein 1 *(CRBP1*), aldehyde dehydrogenase, member 1a2 (*ALDH1A2*) and cytochrome P-450 enzyme (*CYP26A1)*. *RARβ2 (Gillespie and Gudas, 2007)*, *CRBP1* (Smith et al., 1991) and *Cyp26a1 (Ray et al., 1997)* have retinoic acid responsive elements (RAREs) in their promoters, and therefore transcript levels of these genes provide a reliable indicator of tissue retinoid signaling.

Our q-PCR analyses showed that renal transcript levels of *RARα* were unchanged across all groups (Figure 6M). However, transcripts of *RARβ2, RARγ* and *CRBP1* were reduced in HFD-fed mice compared to controls (Figure 6N,O,P, **p*<0.05). Renal transcripts of *ALDH1A2* were unchanged across all groups (Figure 6Q), and, compared to control mice, mean renal levels of *CYP26A1* mRNA were ~2.0-fold lower in HFD-fed mice; however, these differences were not statistically significant (Figure 6R, ns, *p*>0.05).

In HFD+AC261 treated mice, renal transcripts of *RARβ2* were also reduced compare to controls (Figure 6N, **p*<0.05), but higher (~2.5-fold) (Figure 6N, **p*<0.05), than renal *RARβ2* transcript levels of HFD-fed mice. Compared to controls, renal transcript levels of *RARγ* and *CRBP1* were unchanged in HFD+AC261 treated mice

(Figure 6O,P), but, similar to *RARβ2, RARγ* and *CRBP1* transcript levels were significantly higher (~1.8 and ~2.3-fold respectively) than the levels of these genes detected in HFD-fed mice (Figure 6 O, P, *p<0.05). Similarly, renal transcript levels of *CYP26A1* in HFD+AC261 treated mice were ~2.3-fold higher than in HFD-fed mice; however, these differences did not reach the level of statistical significance (Figure 6R, ns, p>0.05).

We next measured renal retinol (ROL) levels by high performance liquid chromatography (HPLC). We found that relative to control mice, HFD and HFD+AC261 treated mice showed approximately 23% and 44% reductions in renal ROL levels, respectively; however, these changes were not statistically significant (Supplemental Figure 1A, ns, p>0.05), nor were renal ROL levels between HFD and HFD+AC261 treated mice (Supplemental Figure 1A, ns, p>0.05). The trends are consistent with our previous research demonstrating that HFD-driven obesity is associated with tissue reductions in retinoids (Trasino et al., 2015). We also measured serum ROL by HPLC. These analyses showed that HFD and HFD+AC261 treated mice had elevations in serum retinol compared to control mice (Supplemental Figure 1B, *p<0.05), but as expected and as we observed with renal ROL levels, no differences in serum ROL was detected between HFD and HFD+AC261 treated mice (Supplemental Figure 1B, ns, p>0.05).

RARβ2 Agonist Improves Renal Lesions in BKS-db/db Mice. Next we examined if AC261 affected histological markers of DN in renal tissue from 16-week-old BKS-db/db (BKS-db) mice treated with AC261 for 14 days. BKS-db mice spontaneously develop obesity and severe insulin resistance, and recapitulate many of the renal histological

changes observed in human DN (Sharma et al., 2003; Brosius et al., 2009). BKS-db mice had significantly elevated body weight (BW) and severe glucose intolerance compared to Wt controls (Supplemental Figure 2A-C, ***p<0.001). BWs from BKS-db mice treated with AC261 for 14 days were similar to untreated BKS-db mice (Supplemental Figure 2A), but AC261 treatments did improve random glucose levels (Supplemental Figure 2B, **p<0.01), glucose tolerance, and area under the curve glucose levels (Supplemental Figure 2C,D, *p<0.05). Our analyses of the pharmacokinetics of AC261 after a single dose show that this drug has excellent properties in terms of half-life and blood levels (Supplemental Figure 3).

Compared to Wt controls, BKS-db had 3.0-fold increased mean glomerular area (Figure 7A [H&E, b vs. a]; 7B, ****p<0.0001), evidence of moderate to severe thickening of the GBM, and prominent PAS positive staining in the GBM of the capillary loops (Figure 7A [PAS, e vs. d, red arrows]; 7C, *p<0.05). Similar to our findings in the HFD-DN cohort, by renal histology evaluation of BKS-db+AC261 treated mice, we found a mitigation of DN lesions compared to untreated BKS-db/db mice; BKS-db+AC261 treated mice showed ~1.4-fold smaller mean glomerular area (Figure 7A [H&E, c vs. b]; 7B, ****p<0.0001) and less mesangial cellularity and expansion, marked by diminished PAS positive material in the mesangium (Figure 7A [PAS, f vs. e, red arrows]; 7C *p<0.05) and capillary loop GBM (Figure 7A [PAS, f vs. e, red arrows]). Consistent with this, GBM thickness in BKS-db+AC261 mice was less pronounced than in untreated BKS-db mice and more closely resembled that seen in wt controls (Figure 7A [PAS, f vs. e and d, red arrows]). We next measured renal podocin protein by IHC and found that, compared to wt controls, untreated BKS-db/db mice showed reduced podocin

staining within the glomerular loops, mesangium and GBM (Figure 7D,E, ***p<0.001). In contrast to untreated BKS-db mice, BKS-db+AC261 mice had increased glomerular podocin protein (Figure 7D,E, **p<0.01). Taken together, these data demonstrate that AC261 possesses therapeutic properties in a HFD-DN model, and can inhibit development of DN histological lesions in the BKS-db genetic model of DN.

DISCUSSION.

RARβ has four known isoforms (1-4) (Zelent et al., 1991; Gudas, 2011), with RARβ2 considered the most prominent during kidney and vertebrate development (Zelent et al., 1991). We previously reported that AC261066, a highly selective agonist for RARβ2 (Lund et al., 2005), possesses glucose-lowering properties in dietary and genetic models of obesity and T2D (Trasino et al., 2016b; Trasino et al., 2016a). In this study we confirm those findings and now report that AC261 diminishes the severity of urine albumin excretion and improves a number of the structural and pathological hallmarks of DN (Brosius et al., 2009; Deji et al., 2009) in HFD-fed mice, including glomerular hypertrophy, mesangial expansion, GBM thickening, and podocyte effacement.

To date no studies have examined the renal protective effects of RA or RAR agonists in a HFD-driven model of DN or in BKS-db mice (Hummel et al., 1966), a frequently used genetic DN model that closely recapitulates a number of features of human DN (Sharma et al., 2003). Still, our findings are consistent with two published rodent DN studies by Kim *et. al* (Kim et al., 2015) and Han *et. al* (Han et al., 2004), demonstrating that RA, a pan-RAR agonist, can mitigate DN progression, proteinuria, and podocyte expression of inflammatory markers in an inbred, genetic rat model of T2D (Kim et al., 2015), and a streptozotocin-induced model of DN (Han et al., 2004) respectively. Our findings elaborate on these RA-DN studies and collectively demonstrate that the therapeutic properties of AC261 are multi-modal, affecting a number of pathways relevant to DN. Of these, the podocyte preserving effect of AC261 may be the most relevant given the central role of podocyte injury in the pathogenesis of

DN and a number of chronic kidney diseases (CKD) (Johnstone and Holzman, 2006; Dronavalli et al., 2008). Furthermore, as we detected anti-DN effects of AC261 in both a dietary (HFD) and a genetic (chow-fed BKS-db mice) obesity model of DN, the renal protective properties of AC261 appear to be independent of diet (*i.e.* BKS-db mice develop DN on chow), which may have particular therapeutic relevance as DN cases disproportionally occur in adults with poorly controlled obesity due to complex interaction of multiple etiologies, including genetic, dietary and other environmental factors (Stenvinkel et al., 2013).

In the larger context of retinoid-CKD research, our findings highlight for the first time a potential role for RARβ2 in CKD, while the vast of majority of retinoid-CKD research has focused on a role for RARα, and the renal protective properties of RARα agonists (Lehrke et al., 2002; Ratnam et al., 2011; Zhong et al., 2011; Mallipattu and He, 2015; Dai et al., 2017). In our HFD-DN study, we did not detect changes to renal transcript levels of *RARα* across all experimental groups, but we did measure significant reductions in *RARβ2*, *RARγ*, and *CRBP1* renal mRNA levels in HFD-fed mice. The trends of these findings are in agreement with a study by Ratnam *et al.* (Ratnam et al., 2011) which demonstrated that renal levels of RARβ, but not RARα, are reduced in the CKD HIV-associated nephropathy (HIVAN) (Ratnam et al., 2011), despite evidence that RARα and RARα agonists are relevant to both the pathogenesis and treatment of HIVAN (Ratnam et al., 2011; Dai et al., 2017) and other CKDs (Ratnam et al., 2011; Zhong et al., 2011; Mallipattu and He, 2015). Our data, coupled to the Ratnam *et al.* (Ratnam et al., 2011) study, suggest that RARβ and its major isoform RARβ2 potentially have an unappreciated role in CKD. Further support for this comes from a study

demonstrating that the anti-CKD and podocyte-preserving effect of highly selective RARα agonists correlates with an increase in podocyte expression of RARβ only (Zhong et al., 2011). Thus, it is our view that not unlike during nephrogenesis (Batourina et al., 2001), where only mice lacking both RARβ2 and RARα develop post-natal renal malformations similar to those observed in VA deficient adult mice (Batourina et al., 2001), a more nuanced and complex involvement of both RARβ2 and RARα likely occurs in adult renal biology, and possibly in DN and other CKDs.

In this study we detected a significantly elevated serum ROL, with concomitant reductions to renal retinol (ROL) levels and to *RARβ2* mRNA in HFD-fed mice compared to control mice. These findings are consistent with multiple lines of evidence of aberrant renal retinoid homeostasis in DN (Raila et al., 2007; Frey et al., 2008; Starkey et al., 2010; Jing et al., 2016), and our previous research (Trasino et al., 2015) where we demonstrated that even with sufficient dietary VA and elevated serum ROL, renal and numerous tissue have marked reductions in retinoid levels and retinoid signaling (Trasino et al., 2015), suggesting that obesity and its related disorders such as DN, may lead to a state of tissue retinoid resistance (Trasino et al., 2015). It is noteworthy to highlight that renal retinoid resistance has been previously documented by our laboratory and others in human renal cancer (RC) (Guo et al., 2001), which show a distinct resistance to the therapeutic effects of retinoids due to loss of RARβ2 expression (reviewed in (Tang and Gudas, 2011), and that reestablishing RARβ2 expression in RC (Touma et al., 2005) restores sensitivity to the anti-tumor effects of retinoids (Touma et al., 2005; Tang and Gudas, 2011). As RARβ2 associated retinoid resistance has been documented in numerous cancers (Tang and Gudas, 2011), these

data collectively suggest that RARβ2 may be necessary for potentiation of global retinoid responsiveness in the kidney and other tissues. This theory is further supported by studies of individuals with non-functional variants of RARβ that develop Matthew-Wood syndrome (MWS) (Srour et al., 2013), a rare genetic disorder that manifests as a severe VA deficient state, also seen in individuals with mutations to *STRA6,* the receptor for RBP4 (Pasutto et al., 2007). MWS manifests as multiple organ malformations including renal dysplasia (Pasutto et al., 2007) and resistance to the effects of exogenous RA and retinoids (Srour et al., 2013).

Whether RARβ2 is involved in the altered retinoid metabolism in DN and CKD remains unclear, as is the mechanism by which renal ROL, retinoid homeostasis and RAR signaling are altered in obesity and DN (Raila et al., 2007; Frey et al., 2008; Starkey et al., 2010; Jing et al., 2016). Nevertheless, if as in RC, RARβ is necessary for cellular RA responsiveness in DN and CKD, our data demonstrating significantly higher renal mRNA levels of *RARβ2, RARγ, CRBP1* in HFD+AC261 treated mice compared to HFD-fed mice is noteworthy and collectively suggest that AC261 treatment engages retinoid pathways and prevents or reverses the reductions of renal retinoid signaling in HFD-fed mice. Compared to HFD-fed mice, we did not detect changes to renal or serum ROL in HFD+AC261 treated mice, suggesting that AC261 may facilitate the utilization of existing renal VA pools or directly transduce retinoid signaling as a RARβ2 selective agonist without raising tissue levels of VA or affected whole body retinoid status. This may be one of the mechanisms by which AC261 discharges its podocyte preserving effect, as podocytes are highly dependent on and sensitive to maintaining endogenous retinoid signaling for function and in response to injury (Suzuki et al., 2003; Peired et al.,

2013). These data warrant further studies to determine if AC261 can potentiate the effects of exogenous retinoids and selective RARα agonists on podocyte function and responses in DN and other CKDs. In the current study, we did not measure renal protein expression of RARβ or RARβ2, as validation studies of commercially available anti-mouse RARβ and RARβ2 antibodies performed in our laboratory demonstrated a lack of specificity (unpublished).

We would also highlight that we previously demonstrated that AC261 possesses lipid-lowering properties in the kidney and other tissues in a HFD-induced T2D mouse model (Trasino et al., 2016a), and this current study expands on those findings and demonstrates that AC261 treatment results in less renal lipid droplet (LD) accumulation in podocytes and endothelial cells (EC); two cell types central to renal function and renal pathology in DN (Johnstone and Holzman, 2006; Dronavalli et al., 2008). Excessive renal LDs have been reported in human obesity, DN, and other renal disease (Bobulescu et al., 2014; Herman-Edelstein et al., 2014), and as such, the “lipotoxicity” hypothesis of DN (reviewed in (Bobulescu, 2010; Herman-Edelstein et al., 2014)), is supported by convincing evidence that ectopic renal LDs can initiate renal inflammatory and fibrotic responses which contribute to podocyte injury and loss (Bobulescu, 2010; Herman-Edelstein et al., 2014). Thus, the concomitant lower LD accumulation and decreases in effacement and injury in podocytes and ECs in HFD+AC261 treated mice compared to HFD-fed mice may be mechanistically related as podocytes and ECs synthesize and maintain components of the protein meshwork of the glomerular basement membrane (Abrahamson, 2012).

As the molecular pathogenesis of T2D and DN is intimately intertwined, and as podocytes are insulin-sensitive and hyperglycemia can induce podocyte injury (Coward and Saleem, 2011; Jain et al., 2011), we recognize that additional studies using mouse models with tissue and/or cell-specific RARβ and RARβ2 ablation are warranted to determine if the therapeutic effects of AC261 in the kidney result from direct drug actions on several renal cell types or via indirect effects related to AC261's glucose-lowering properties. However, clinical data show that intensive glycemic and hypertension control has limited therapeutic effectiveness for DN (Parving et al., 2012; Fried et al., 2013; Gentile et al., 2014; Hajhosseiny et al., 2014). Additional studies are also needed to determine if AC261 can reverse renal damage associated with DN since in this work we are measuring the ability of the drug to inhibit the development of DN.

While these results are promising, we recognize that one of the limitations of this pre-clinical study is the number of mice used. Future studies using larger cohorts of mice to measure effects of AC261 on clinical and molecular pathways related to DN are planned. Nevertheless, given the lack of FDA-approved DN therapies, from a drug-development perspective these proof of concept, pre-clinical studies of the therapeutic properties of the RARβ2 agonist AC261 are promising, as AC261 is orally bioavailable (Lund et al., 2005; Trasino et al., 2016b), does not result in unwanted weight-gain in the mouse models, and does not show any observable adverse effects in acute or long-term administration in rodents (Trasino et al., 2016b; Trasino et al., 2016a).

ACKNOWLEDGEMENTS.

We thank Viral Patel for urine albumin and creatinine analysis, the Gudas lab members for data discussions, Daniel Stummer for editorial assistance, and the Weill Cornell Electron Microscopy Core Laboratory for TEM tissue processing, image acquisition and analysis.

AUTHORSHIP CONTRIBUTIONS.

Participated in research design: SET, XHT, MMS, MEC, & LJG.

Conducted experiments: SET, XHT, & LJG.

Performed data analysis: SET, XHT, MMS, MEC, & LJG.

Wrote or contributed to the writing of the manuscript: SET, XHT, MMS, MEC, & LJG.

CONFLICT OF INTEREST.

Weill Cornell has filed a patent on some of the intellectual property in this manuscript. This patent was licensed to Sveikatal, Inc. LJG and XHT are founders of Sveikatal, Inc., and LJG, XHT, and SET are named on the patent.

REFERENCES.

Abrahamson DR (2012) Role of the podocyte (and glomerular endothelium) in building the GBM. *Semin Nephrol* **32**:342-349.

Alsaad KO and Herzenberg AM (2007) Distinguishing diabetic nephropathy from other causes of glomerulosclerosis: an update. *J Clin Pathol* **60**:18-26.

Anderson RJ, Ray CJ and Hattler BG (1998) Retinoic acid regulation of renal tubular epithelial and vascular smooth muscle cell function. *J Am Soc Nephrol* **9**:773-781.

Batourina E, Choi C, Paragas N, Bello N, Hensle T, Costantini FD, Schuchardt A, Bacallao RL and Mendelsohn CL (2002) Distal ureter morphogenesis depends on epithelial cell remodeling mediated by vitamin A and Ret. *Nat Genet* **32**:109-115.

Batourina E, Gim S, Bello N, Shy M, Clagett-Dame M, Srinivas S, Costantini F and Mendelsohn C (2001) Vitamin A controls epithelial/mesenchymal interactions through Ret expression. *Nat Genet* **27**:74-78.

Blomhoff R, Green MH, Berg T and Norum KR (1990) Transport and storage of vitamin A. *Science* **250**:399-404.

Bobulescu IA (2010) Renal lipid metabolism and lipotoxicity. *Curr Opin Nephrol Hypertens* **19**:393-402.

Bobulescu IA, Lotan Y, Zhang J, Rosenthal TR, Rogers JT, Adams-Huet B, Sakhaee K and Moe OW (2014) Triglycerides in the human kidney cortex: relationship with body size. *PLoS One* **9**:e101285.

Bollig F, Perner B, Besenbeck B, Köthe S, Ebert C, Taudien S and Englert C (2009) A highly conserved retinoic acid responsive element controls wt1a expression in the zebrafish pronephros. *Development* **136**:2883-2892.

Brosius FC, Alpers CE, Bottinger EP, Breyer MD, Coffman TM, Gurley SB, Harris RC, Kakoki M, Kretzler M, Leiter EH, Levi M, McIndoe RA, Sharma K, Smithies O, Susztak K, Takahashi N, Takahashi T and Consortium AMoDC (2009) Mouse models of diabetic nephropathy. *J Am Soc Nephrol* **20**:2503-2512.

Chambon P (1996) A decade of molecular biology of retinoic acid receptors. *FASEB J* **10**:940-954.

Chiba T, Skrypnyk NI, Skvarca LB, Penchev R, Zhang KX, Rochon ER, Fall JL, Paueksakon P, Yang H, Alford CE, Roman BL, Zhang MZ, Harris R, Hukriede NA and de Caestecker MP (2016) Retinoic Acid Signaling Coordinates Macrophage-Dependent Injury and Repair after AKI. *J Am Soc Nephrol* **27**:495-508.

Cook HT (2010) The origin of renal fibroblasts and progression of kidney disease. *Am J Pathol* **176**:22-24.

Couchman JR, Beavan LA and McCarthy KJ (1994) Glomerular matrix: synthesis, turnover and role in mesangial expansion. *Kidney Int* **45**:328-335.

Coward RJ and Saleem MA (2011) Podocytes as a target of insulin. *Curr Diabetes Rev* **7**:22-27.

Dai Y, Chen A, Liu R, Gu L, Sharma S, Cai W, Salem F, Salant DJ, Pippin JW, Shankland SJ, Moeller MJ, Ghyselinck NB, Ding X, Chuang PY, Lee K and He JC (2017) Retinoic acid improves nephrotoxic serum-induced glomerulonephritis through activation of podocyte retinoic acid receptor α. *Kidney Int* **92**:1444-1457.

de Boer IH, Rue TC, Hall YN, Heagerty PJ, Weiss NS and Himmelfarb J (2011) Temporal trends in the prevalence of diabetic kidney disease in the United States. *JAMA* **305**:2532-2539.

Deegens JK, Dijkman HB, Borm GF, Steenbergen EJ, van den Berg JG, Weening JJ and Wetzels JF (2008) Podocyte foot process effacement as a diagnostic tool in focal segmental glomerulosclerosis. *Kidney Int* **74**:1568-1576.

Deji N, Kume S, Araki S, Soumura M, Sugimoto T, Isshiki K, Chin-Kanasaki M, Sakaguchi M, Koya D, Haneda M, Kashiwagi A and Uzu T (2009) Structural and functional changes in the kidneys of high-fat diet-induced obese mice. *Am J Physiol Renal Physiol* **296**:F118-126.

Dong L, Pietsch S, Tan Z, Perner B, Sierig R, Kruspe D, Groth M, Witzgall R, Gröne HJ, Platzer M and Englert C (2015) Integration of Cistromic and Transcriptomic Analyses Identifies Nphs2, Mafb, and Magi2 as Wilms' Tumor 1 Target Genes in Podocyte Differentiation and Maintenance. *J Am Soc Nephrol* **26**:2118-2128.

Dronavalli S, Duka I and Bakris GL (2008) The pathogenesis of diabetic nephropathy. *Nat Clin Pract Endocrinol Metab* **4**:444-452.

Frey SK, Nagl B, Henze A, Raila J, Schlosser B, Berg T, Tepel M, Zidek W, Weickert MO, Pfeiffer AF and Schweigert FJ (2008) Isoforms of retinol binding protein 4 (RBP4) are increased in chronic diseases of the kidney but not of the liver. *Lipids Health Dis* **7**:29.

Fried LF, Emanuele N, Zhang JH, Brophy M, Conner TA, Duckworth W, Leehey DJ, McCullough PA, O'Connor T, Palevsky PM, Reilly RF, Seliger SL, Warren SR, Watnick S, Peduzzi P, Guarino P and Investigators VN-D (2013) Combined angiotensin inhibition for the treatment of diabetic nephropathy. *N Engl J Med* **369**:1892-1903.

Gentile G, Mastroluca D, Ruggenenti P and Remuzzi G (2014) Novel effective drugs for diabetic kidney disease? or not? *Expert Opin Emerg Drugs* **19**:571-601.

Gilbert T (2002) Vitamin A and kidney development. *Nephrol Dial Transplant* **17 Suppl 9**:78-80.

Gillespie RF and Gudas LJ (2007) Retinoid regulated association of transcriptional co-regulators and the polycomb group protein SUZ12 with the retinoic acid response elements of Hoxa1, RARbeta(2), and Cyp26A1 in F9 embryonal carcinoma cells. *J Mol Biol* **372**:298-316.

Gudas LJ (2011) Emerging roles for retinoids in regeneration and differentiation in normal and disease states. *Biochim Biophys Acta*.

Gudas LJ (2012) Emerging roles for retinoids in regeneration and differentiation in normal and disease states. *Biochim Biophys Acta* **1821**:213-221.

Guo M, Ricardo SD, Deane JA, Shi M, Cullen-McEwen L and Bertram JF (2005) A stereological study of the renal glomerular vasculature in the db/db mouse model of diabetic nephropathy. *J Anat* **207**:813-821.

Guo X, Nanus DM, Ruiz A, Rando RR, Bok D and Gudas LJ (2001) Reduced levels of retinyl esters and vitamin A in human renal cancers. *Cancer Res* **61**:2774-2781.

Hajhosseiny R, Khavandi K, Jivraj N, Mashayekhi S, Goldsmith DJ and Malik RA (2014) Have we reached the limits for the treatment of diabetic nephropathy? *Expert Opin Investig Drugs* **23**:511-522.

Han SY, So GA, Jee YH, Han KH, Kang YS, Kim HK, Kang SW, Han DS, Han JY and Cha DR (2004) Effect of retinoic acid in experimental diabetic nephropathy. *Immunol Cell Biol* **82**:568-576.

Hartwig S, Ho J, Pandey P, Macisaac K, Taglienti M, Xiang M, Alterovitz G, Ramoni M, Fraenkel E and Kreidberg JA (2010) Genomic characterization of Wilms' tumor suppressor 1 targets in nephron progenitor cells during kidney development. *Development* **137**:1189-1203.

Herman-Edelstein M, Scherzer P, Tobar A, Levi M and Gafter U (2014) Altered renal lipid metabolism and renal lipid accumulation in human diabetic nephropathy. *J Lipid Res* **55**:561-572.

Hummel KP, Dickie MM and Coleman DL (1966) Diabetes, a new mutation in the mouse. *Science* **153**:1127-1128.

Jain S, De Petris L, Hoshi M, Akilesh S, Chatterjee R and Liapis H (2011) Expression profiles of podocytes exposed to high glucose reveal new insights into early diabetic glomerulopathy. *Lab Invest* **91**:488-498.

Jensen EB, Gundersen HJ and Osterby R (1979) Determination of membrane thickness distribution from orthogonal intercepts. *J Microsc* **115**:19-33.

Jing J, Isoherranen N, Robinson-Cohen C, Petrie I, Kestenbaum BR and Yeung CK (2016) Chronic Kidney Disease Alters Vitamin A Homeostasis via Effects on Hepatic RBP4 Protein Expression and Metabolic Enzymes. *Clin Transl Sci* **9**:207-215.

Johnstone DB and Holzman LB (2006) Clinical impact of research on the podocyte slit diaphragm. *Nat Clin Pract Nephrol* **2**:271-282.

Kang HM, Ahn SH, Choi P, Ko YA, Han SH, Chinga F, Park AS, Tao J, Sharma K, Pullman J, Bottinger EP, Goldberg IJ and Susztak K (2015) Defective fatty acid oxidation in renal tubular epithelial cells has a key role in kidney fibrosis development. *Nat Med* **21**:37-46.

Kawachi H, Miyauchi N, Suzuki K, Han GD, Orikasa M and Shimizu F (2006) Role of podocyte slit diaphragm as a filtration barrier. *Nephrology (Carlton)* **11**:274-281.

Kim CS, Park JS, Ahn CW and Kim KR (2015) All-Trans Retinoic Acid Has a Potential Therapeutic Role for Diabetic Nephropathy. *Yonsei Med J* **56**:1597-1603.

Konoshita T, Wakahara S, Mizuno S, Motomura M, Aoyama C, Makino Y, Kawai Y, Kato N, Koni I, Miyamori I and Mabuchi H (2006) Tissue gene expression of renin-angiotensin system in human type 2 diabetic nephropathy. *Diabetes Care* **29**:848-852.

Kreidberg JA, Sariola H, Loring JM, Maeda M, Pelletier J, Housman D and Jaenisch R (1993) WT-1 is required for early kidney development. *Cell* **74**:679-691.

Krendel M, Kim SV, Willinger T, Wang T, Kashgarian M, Flavell RA and Mooseker MS (2009) Disruption of Myosin 1e promotes podocyte injury. *J Am Soc Nephrol* **20**:86-94.

Kurien BT and Scofield RH (1999) Mouse urine collection using clear plastic wrap. *Lab Anim* **33**:83-86.

Lasagni L, Angelotti ML, Ronconi E, Lombardi D, Nardi S, Peired A, Becherucci F, Mazzinghi B, Sisti A, Romoli S, Burger A, Schaefer B, Buccoliero A, Lazzeri E and Romagnani P (2015) Podocyte Regeneration Driven by Renal Progenitors Determines Glomerular Disease Remission and Can Be Pharmacologically Enhanced. *Stem Cell Reports* **5**:248-263.

Lazzeri E, Peired AJ, Lasagni L and Romagnani P (2014) Retinoids and glomerular regeneration. *Semin Nephrol* **34**:429-436.

Lehrke I, Schaier M, Schade K, Morath C, Waldherr R, Ritz E and Wagner J (2002) Retinoid receptor-specific agonists alleviate experimental glomerulonephritis. *Am J Physiol Renal Physiol* **282**:F741-751.

Lelièvre-Pégorier M, Vilar J, Ferrier ML, Moreau E, Freund N, Gilbert T and Merlet-Bénichou C (1998) Mild vitamin A deficiency leads to inborn nephron deficit in the rat. *Kidney Int* **54**:1455-1462.

Livak KJ and Schmittgen TD (2001) Analysis of relative gene expression data using real-time quantitative PCR and the 2(-Delta Delta C(T)) Method. *Methods* **25**:402-408.

Lu TC, Wang Z, Feng X, Chuang P, Fang W, Chen Y, Neves S, Maayan A, Xiong H, Liu Y, Iyengar R, Klotman PE and He JC (2008) Retinoic acid utilizes CREB and USF1 in a transcriptional feed-forward loop in order to stimulate MKP1 expression in human immunodeficiency virus-infected podocytes. *Mol Cell Biol* **28**:5785-5794.

Lund BW, Knapp AE, Piu F, Gauthier NK, Begtrup M, Hacksell U and Olsson R (2009) Design, synthesis, and structure-activity analysis of isoform-selective retinoic acid receptor beta ligands. *J Med Chem* **52**:1540-1545.

Lund BW, Piu F, Gauthier NK, Eeg A, Currier E, Sherbukhin V, Brann MR, Hacksell U and Olsson R (2005) Discovery of a potent, orally available, and isoform-selective retinoic acid beta2 receptor agonist. *J Med Chem* **48**:7517-7519.

Mallipattu SK and He JC (2015) The beneficial role of retinoids in glomerular disease. *Front Med (Lausanne)* **2**:16.

Manzano VM, Muñoz JC, Jiménez JR, Puyol MR, Puyol DR, Kitamura M and Cazaña FJ (2000) Human renal mesangial cells are a target for the anti-inflammatory action of 9-cis retinoic acid. *Br J Pharmacol* **131**:1673-1683.

Mendelsohn C, Batourina E, Fung S, Gilbert T and Dodd J (1999) Stromal cells mediate retinoid-dependent functions essential for renal development. *Development* **126**:1139-1148.

Nagata M (2016) Podocyte injury and its consequences. *Kidney Int* **89**:1221-1230.

Nakamura T, Ushiyama C, Suzuki S, Hara M, Shimada N, Ebihara I and Koide H (2000) Urinary excretion of podocytes in patients with diabetic nephropathy. *Nephrol Dial Transplant* **15**:1379-1383.

Palmer RE, Kotsianti A, Cadman B, Boyd T, Gerald W and Haber DA (2001) WT1 regulates the expression of the major glomerular podocyte membrane protein Podocalyxin. *Curr Biol* **11**:1805-1809.

Parving HH, Brenner BM, McMurray JJ, de Zeeuw D, Haffner SM, Solomon SD, Chaturvedi N, Persson F, Desai AS, Nicolaides M, Richard A, Xiang Z, Brunel P, Pfeffer MA and Investigators A (2012) Cardiorenal end points in a trial of aliskiren for type 2 diabetes. *N Engl J Med* **367**:2204-2213.

Pasutto F, Sticht H, Hammersen G, Gillessen-Kaesbach G, Fitzpatrick DR, Nürnberg G, Brasch F, Schirmer-Zimmermann H, Tolmie JL, Chitayat D, Houge G, Fernández-Martínez L, Keating S, Mortier G, Hennekam RC, von der Wense A, Slavotinek A, Meinecke P, Bitoun P, Becker C, Nürnberg P, Reis A and Rauch A (2007) Mutations in STRA6 cause a broad spectrum of malformations including anophthalmia, congenital heart defects, diaphragmatic hernia, alveolar capillary dysplasia, lung hypoplasia, and mental retardation. *Am J Hum Genet* **80**:550-560.

Peired A, Angelotti ML, Ronconi E, la Marca G, Mazzinghi B, Sisti A, Lombardi D, Giocaliere E, Della Bona M, Villanelli F, Parente E, Ballerini L, Sagrinati C, Wanner N, Huber TB, Liapis H, Lazzeri E, Lasagni L and Romagnani P (2013) Proteinuria impairs podocyte regeneration by sequestering retinoic acid. *J Am Soc Nephrol* **24**:1756-1768.

Perez A, Ramirez-Ramos M, Calleja C, Martin D, Namorado MC, Sierra G, Ramirez-Ramos ME, Paniagua R, Sánchez Y, Arreola L and Reyes JL (2004) Beneficial effect of retinoic acid on the outcome of experimental acute renal failure. *Nephrol Dial Transplant* **19**:2464-2471.

Raila J, Henze A, Spranger J, Möhlig M, Pfeiffer AF and Schweigert FJ (2007) Microalbuminuria is a major determinant of elevated plasma retinol-binding protein 4 in type 2 diabetic patients. *Kidney Int* **72**:505-511.

Raila J, Willnow TE and Schweigert FJ (2005) Megalin-mediated reuptake of retinol in the kidneys of mice is essential for vitamin A homeostasis. *J Nutr* **135**:2512-2516.

Ratnam KK, Feng X, Chuang PY, Verma V, Lu TC, Wang J, Jin Y, Farias EF, Napoli JL, Chen N, Kaufman L, Takano T, D'Agati VD, Klotman PE and He JC (2011) Role of the retinoic acid receptor-α in HIV-associated nephropathy. *Kidney Int* **79**:624-634.

Ray WJ, Bain G, Yao M and Gottlieb DI (1997) CYP26, a novel mammalian cytochrome P450, is induced by retinoic acid and defines a new family. *J Biol Chem* **272**:18702-18708.

Rosselot C, Spraggon L, Chia I, Batourina E, Riccio P, Lu B, Niederreither K, Dolle P, Duester G, Chambon P, Costantini F, Gilbert T, Molotkov A and Mendelsohn C (2010) Non-cell-autonomous retinoid signaling is crucial for renal development. *Development* **137**:283-292.

Sagrinati C, Netti GS, Mazzinghi B, Lazzeri E, Liotta F, Frosali F, Ronconi E, Meini C, Gacci M, Squecco R, Carini M, Gesualdo L, Francini F, Maggi E, Annunziato F, Lasagni L, Serio M, Romagnani S and Romagnani P (2006) Isolation and characterization of multipotent progenitor cells from the Bowman's capsule of adult human kidneys. *J Am Soc Nephrol* **17**:2443-2456.

Sastre C, Rubio-Navarro A, Buendía I, Gómez-Guerrero C, Blanco J, Mas S, Egido J, Blanco-Colio LM, Ortiz A and Moreno JA (2013) Hyperlipidemia-associated renal damage decreases Klotho expression in kidneys from ApoE knockout mice. *PLoS One* **8**:e83713.

Schaier M, Lehrke I, Schade K, Morath C, Shimizu F, Kawachi H, Grone HJ, Ritz E and Wagner J (2001) Isotretinoin alleviates renal damage in rat chronic glomerulonephritis. *Kidney Int* **60**:2222-2234.

Schindelin J, Arganda-Carreras I, Frise E, Kaynig V, Longair M, Pietzsch T, Preibisch S, Rueden C, Saalfeld S, Schmid B, Tinevez JY, White DJ, Hartenstein V, Eliceiri K, Tomancak P and Cardona A (2012) Fiji: an open-source platform for biological-image analysis. *Nat Methods* **9**:676-682.

Sharma K, McCue P and Dunn SR (2003) Diabetic kidney disease in the db/db mouse. *Am J Physiol Renal Physiol* **284**:F1138-1144.

Smith FR and Goodman DS (1971) The effects of diseases of the liver, thyroid, and kidneys on the transport of vitamin A in human plasma. *J Clin Invest* **50**:2426-2436.

Smith WC, Nakshatri H, Leroy P, Rees J and Chambon P (1991) A retinoic acid response element is present in the mouse cellular retinol binding protein I (mCRBPI) promoter. *EMBO J* **10**:2223-2230.

Srour M, Chitayat D, Caron V, Chassaing N, Bitoun P, Patry L, Cordier MP, Capo-Chichi JM, Francannet C, Calvas P, Ragge N, Dobrzeniecka S, Hamdan FF, Rouleau GA, Tremblay A and Michaud JL (2013) Recessive and dominant

mutations in retinoic acid receptor beta in cases with microphthalmia and diaphragmatic hernia. *Am J Hum Genet* **93**:765-772.

Starkey JM, Zhao Y, Sadygov RG, Haidacher SJ, Lejeune WS, Dey N, Luxon BA, Kane MA, Napoli JL, Denner L and Tilton RG (2010) Altered retinoic acid metabolism in diabetic mouse kidney identified by O isotopic labeling and 2D mass spectrometry. *PLoS One* **5**:e11095.

Stenvinkel P, Zoccali C and Ikizler TA (2013) Obesity in CKD--what should nephrologists know? *J Am Soc Nephrol* **24**:1727-1736.

Stratton IM, Adler AI, Neil HA, Matthews DR, Manley SE, Cull CA, Hadden D, Turner RC and Holman RR (2000) Association of glycaemia with macrovascular and microvascular complications of type 2 diabetes (UKPDS 35): prospective observational study. *BMJ* **321**:405-412.

Su B, Chen X, Zhong C, Guo N, He J and Fan Y (2012) All-trans retinoic acid inhibits mesangial cell proliferation by up-regulating p21Waf1/Cip1 and p27Kip1 and down-regulating Skp2. *J Nephrol* **25**:1031-1040.

Suzuki A, Ito T, Imai E, Yamato M, Iwatani H, Kawachi H and Hori M (2003) Retinoids regulate the repairing process of the podocytes in puromycin aminonucleoside-induced nephrotic rats. *J Am Soc Nephrol* **14**:981-991.

Szeto HH, Liu S, Soong Y, Seshan SV, Cohen-Gould L, Manichev V, Feldman LC and Gustafsson T (2017) Mitochondria Protection after Acute Ischemia Prevents Prolonged Upregulation of IL-1β and IL-18 and Arrests CKD. *J Am Soc Nephrol* **28**:1437-1449.

Tain YL, Lin YJ, Sheen JM, Yu HR, Tiao MM, Chen CC, Tsai CC, Huang LT and Hsu CN (2017) High Fat Diets Sex-Specifically Affect the Renal Transcriptome and Program Obesity, Kidney Injury, and Hypertension in the Offspring. *Nutrients* **9**.

Tang XH and Gudas LJ (2011) Retinoids, retinoic acid receptors, and cancer. *Annu Rev Pathol* **6**:345-364.

Tervaert TW, Mooyaart AL, Amann K, Cohen AH, Cook HT, Drachenberg CB, Ferrario F, Fogo AB, Haas M, de Heer E, Joh K, Noël LH, Radhakrishnan J, Seshan SV, Bajema IM, Bruijn JA and Society RP (2010) Pathologic classification of diabetic nephropathy. *J Am Soc Nephrol* **21**:556-563.

Touma SE, Goldberg JS, Moench P, Guo X, Tickoo SK, Gudas LJ and Nanus DM (2005) Retinoic acid and the histone deacetylase inhibitor trichostatin a inhibit the proliferation of human renal cell carcinoma in a xenograft tumor model. *Clin Cancer Res* **11**:3558-3566.

Trasino SE, Tang XH, Jessurun J and Gudas LJ (2015) Obesity Leads to Tissue, but not Serum Vitamin A Deficiency. *Sci Rep* **5**:15893.

Trasino SE, Tang XH, Jessurun J and Gudas LJ (2016a) A retinoic acid receptor β2 agonist reduces hepatic stellate cell activation in nonalcoholic fatty liver disease. *J Mol Med (Berl)* **94**:1143-1151.

Trasino SE, Tang XH, Jessurun J and Gudas LJ (2016b) Retinoic acid receptor β2 agonists restore glycaemic control in diabetes and reduce steatosis. *Diabetes Obes Metab* **18**:142-151.

Uhlén M, Fagerberg L, Hallström BM, Lindskog C, Oksvold P, Mardinoglu A, Sivertsson Å, Kampf C, Sjöstedt E, Asplund A, Olsson I, Edlund K, Lundberg E, Navani S, Szigyarto CA, Odeberg J, Djureinovic D, Takanen JO, Hober S, Alm T, Edqvist PH, Berling H, Tegel H, Mulder J, Rockberg J, Nilsson P, Schwenk JM, Hamsten M, von Feilitzen K, Forsberg M, Persson L, Johansson F, Zwahlen M, von Heijne G, Nielsen J and Pontén F (2015) Proteomics. Tissue-based map of the human proteome. *Science* **347**:1260419.

Valmadrid CT, Klein R, Moss SE and Klein BE (2000) The risk of cardiovascular disease mortality associated with microalbuminuria and gross proteinuria in persons with older-onset diabetes mellitus. *Arch Intern Med* **160**:1093-1100.

Vaughan MR, Pippin JW, Griffin SV, Krofft R, Fleet M, Haseley L and Shankland SJ (2005) ATRA induces podocyte differentiation and alters nephrin and podocin expression in vitro and in vivo. *Kidney Int* **68**:133-144.

Wagner J, Dechow C, Morath C, Lehrke I, Amann K, Waldherr R, Floege J and Ritz E (2000) Retinoic acid reduces glomerular injury in a rat model of glomerular damage. *J Am Soc Nephrol* **11**:1479-1487.

Wei P, Lane PH, Lane JT, Padanilam BJ and Sansom SC (2004) Glomerular structural and functional changes in a high-fat diet mouse model of early-stage Type 2 diabetes. *Diabetologia* **47**:1541-1549.

Weibel ER and DM. G (1962) A principle for counting tissue structures on random sections. *J Appl Physiol* **17**:343-348.

Zelent A, Mendelsohn C, Kastner P, Krust A, Garnier JM, Ruffenach F, Leroy P and Chambon P (1991) Differentially expressed isoforms of the mouse retinoic acid receptor beta generated by usage of two promoters and alternative splicing. *EMBO J* **10**:71-81.

Zhang J, Pippin JW, Vaughan MR, Krofft RD, Taniguchi Y, Romagnani P, Nelson PJ, Liu ZH and Shankland SJ (2012) Retinoids augment the expression of podocyte proteins by glomerular parietal epithelial cells in experimental glomerular disease. *Nephron Exp Nephrol* **121**:e23-37.

Zhong Y, Wu Y, Liu R, Li Z, Chen Y, Evans T, Chuang P, Das B and He JC (2011) Novel retinoic acid receptor alpha agonists for treatment of kidney disease. *PLoS One* **6**:e27945.

FOOTNOTES.

This research was supported in part by Weill Cornell funds and the National Institutes of Health National Institute of Diabetes and Digestive and Kidney Diseases (NIDDK) [R01 DK113088] and the National Institutes of Health National Cancer Institute (NCI) [T32 CA062948].

JPET Fast Forward. Published on July 27, 2018 as DOI: 10.1124/jpet.118.249375
This article has not been copyedited and formatted. The final version may differ from this version.

FIGURE LEGENDS

Figure 1. Effects of AC261066 (AC261), a Retinoic Acid Receptor β2 (RARβ2) Agonist, on Glucose Tolerance and Urine Albumin Excretion in a High Fat Dietary Model of Diabetic Nephropathy. A) Body weights of C57BL/6 wt male mice after 16-weeks of being fed either: a standard control chow (13% kcal fat) diet (Con, n=4); a high fat (45% kcal fat) diet (HFD, n=4); or HFD with the RARβ2 agonist, AC261066 (HFD+AC261, n=4) in their drinking water from week 5 to week 16. **B)** Fasting glucose levels in mice from **A)**. **C)** Glucose tolerance tests (GTT) and, **D)** Area under the curve (AUC) glucose in mice from **A)**. **E)** Spot morning urine albumin concentration (μg/mL) and, **F)** Spot morning albumin: creatinine ratio (ACR) in mice described in Materials and Methods, with control mice (n=5); (HFD, n=5); and (HFD+AC261, n=3). Errors bars represent ± SD of the mean with **p*<0.05, ***p*<0.01, ****p*<0.001, *****p*<0.0001.

Figure 2. Retinoic Acid Receptor β2 Agonist Results in Less Tubule Lipid Droplet (LD), Mesangial Expansion, and Glomerular Hypertrophy. A) [a-c] Representative images of Hematoxylin and Eosin (H&E) stained renal tissue analyzed by light microscopy showing glomeruli and tubule LD vacuolization [b and c, yellow arrows], in mice described in Figure 1A and analyzed with control mice (n=4); (HFD, n=4); and (HFD+AC261, n=4). Magnification: 100X; Scale Bars=50 μm. **B)** Tubule vacuolization histology score of all mice from **A)** and as described in Materials and Methods (ND=not detected). **C)** Representative images of Periodic Acid-Schiff (PAS) [a-c; yellow arrows, a-c; capillary glomerular basement membrane (GBM) thickening], and H&E stained [d-f] glomeruli in all mice from **A)**. (Magnification: 400X; Scale Bars=100 μm. **D)** Mesangial

expansion histology score of all mice from **A)** and as described in Materials and Methods. **E)** Mean Glomerular Area (-10^3 μm^2) of all mice from **A)** and as described in Materials and Methods. Histogram individual data points represent the score of each slide analyzed per mouse as described in Materials and Methods. Errors bars represent ± SD of the mean of each group with *p<0.05, **p<0.01, ***p<0.001.

Figure 3. Retinoic Acid Receptor β2 (RARβ2) Agonist-Treated Mice Show Lower Renal α-Smooth Muscle Actin α-SMA and Type IV Collagen Resulting from a HFD. **A)** [a-c] Representative images of α-SMA immunohistochemistry (IHC) performed on renal sections from mice described in Figure 1A with control mice (n=3), (HFD, n=3), and (HFD+AC261, n=3). Magnification: 100X; Scale Bars=50 μm; Inset Dotted Field Magnification: 400X, Scale Bars=100 μm. **B)** α-SMA IHC staining optical density (OD) determined in all mice from **A)** and as described in Materials and Methods. **C)** Collagen IV IHC staining optical density (OD) score in all mice from **A)** and as described in Materials and Methods. **D)** Representative images of collagen IV IHC performed on renal sections from all mice described **A)**. Magnification: 200X; Scale Bars=50 μm. Histogram individual data points represent the score of each slide analyzed per mouse as described in Materials and Methods. Errors bars represent ± SD of the mean of each group with ****p<0.0001.

Figure 4. Less Podocyte Effacement, Glomerular Basement Membrane Thickening, and Ultrastructural Renal Lesions in Retinoic Acid Receptor β2 (RARβ2) Agonist-Treated Mice. A-C) Representative transmission electronic microscopic (TEM) images of glomeruli from mice described in Figure 1A with control

mice (n=3), (HFD, n=3), and (HFD+AC261, n=3). Magnification: 20,000X; Scale Bars=1μm; Indicators: [black arrows=capillary endothelial cell (EC) fenestrations; red arrows=podocyte foot process effacement and collapse; yellow arrows=podocyte and EC lipid droplets (LDs); white arrows=EC collapse; *****(asterisks) = podocyte foot process slit diaphragm; **+** (black cross) = capillary glomerular basement membrane].
D) Representative TEM images of glomerular basement membranes (GBM) from mice described in Figure 1A. Magnification: 20,000X; Scale Bars=1μm; Indicators: [black cross=GBM; red arrow=podocyte foot process effacement and collapse]. **E) and F)** Quantitation of GBM thickness and podocyte foot process density as described in Materials and Methods. Histogram individual data points represent the score of each slide analyzed per mouse as described in Materials and Methods. Errors bars represent ± SD of the mean of each group with ***p*<0.01, *****p*<0.0001.

Figure 5. Effects of Retinoic Acid Receptor β2 (RARβ2) Agonist on Podocin and WT1 Protein Expression. **A)** Representative images of podocin (membranous positivity) **[a-c],** and Wilms' tumor 1 (WT1) (nuclear positivity) **[d-f]** immunohistochemistry (IHC) performed on renal sections from mice described in Figure 1A with control mice (n=4), (HFD, n=4), and (HFD+AC261, n=4). Magnification: 400X; Scale Bars=100 μm. **B)** and **C)** Podocin and WT1 IHC staining optical density (OD) and positive glomerular cell quantitation of all mice from **A)** and as described in Materials and Methods. Histogram individual data points represent the score of each slide analyzed per mouse as described in Materials and Methods. Errors bars represent ± SD of the mean of each group with ***p*<0.01, ****p*<0.001, *****p*<0.0001.

Figure 6. Modulation of Renal, Podocyte, and Vitamin A-Specific Genes by a HFD and Retinoic Acid Receptor β2 (RARβ2) Agonist. Quantitative RT-PCR measurements of relative renal cortex tissue transcript levels of podocyte-specific genes from Wt C57BL/6 male mice fed either chow or HFD diets with and without the RARβ agonist; (control mice, n=4), (HFD, n=4), and (HFD+AC261, n=4) as descried in the Methods. Relative renal mRNA levels of: **A)** Wilms Tumor 1 (*WT-1*), **B)** Podocin (*Nphs2*), **C)** Nephrin (*Nphs1*), **D)** Podocalyxin (*Podxl*), **E)** Synaptopodin (*Synpo*), **F)** Renin (*Ren*), **G)** Angiotensin I Converting Enzyme 1 (*Ace1*), **H)** Angiotensin I Converting Enzyme 2 (*Ace2*), **I)** Bone Morphogenetic Protein 7 (*BMP7*), **J)** Paired box protein Pax-2 (*Pax2*), **K)** MAF BZIP Transcription Factor B (*MafB*), **L)** Ret Proto-Oncogene (*Ret*), **M)** Retinoic Acid Receptor α (RARα*),* **N)** Retinoic Acid Receptor β2 (*RARβ2*), **O)** Retinoic Acid Receptor γ (*RARγ*), **P)** cellular retinoid binding protein 1 (*CRBP1*), **Q)** aldehyde dehydrogenase, member 1a2 (*ALDH1A2*), **R)** cytochrome P-450 enzyme (*Cyp26a1*). Relative fold mRNA levels were normalized to transcript levels of hypoxanthine guanine phosphoribosyl transferase (*Hprt*) and analyzed by the delta, delta CT method as described in Materials and Methods. Histogram individual data points represent the mean of each mouse. Errors bars represent ± SD of the mean of (n=4) animals for each experimental group, with *p<0.05, **p<0.01, ***p<0.001, ****p<0.0001 and ns=not significant.

Figure. 7. RARβ2 Agonist-Treated BKS-db/db Mice Show Fewer DN Lesions. **A)** Representative images of Hematoxylin and Eosin (H&E) [a-c], and Periodic Acid-Schiff (PAS) [d-f, red arrows=capillary glomerular basement membrane thickening] stained renal sections from male Wt C57BL/6 (control, n=4) and 14-week-old BKS-

db/db (BKS-db, n=3) mice fed chow with and without the RARβ2 agonist AC261066 (BKS-db+AC261, n=3) for 14 days. **B)** Mean Glomerular Area (-10^3 μm^2) of mice from **A)**, as described in Materials and Methods. **C)** Mesangial expansion histology score of mice from **A)** and as described in Materials and Methods. **D)** Representative images of podocin immunohistochemistry (IHC) performed on renal sections from mice from **A)**. Magnification: 400X; Scale Bars=100 μm. **E)** Podocin IHC staining optical density (OD) quantitation of mice from **A)** and as described in Materials and Methods. Histogram individual data points represent the score of each slide analyzed per mouse as described in Materials and Methods. Errors bars represent ± SD of the mean of each group with *p<0.05, **p<0.01, ***p<0.001, ****p<0.0001.

Figure 1

JPET#249375

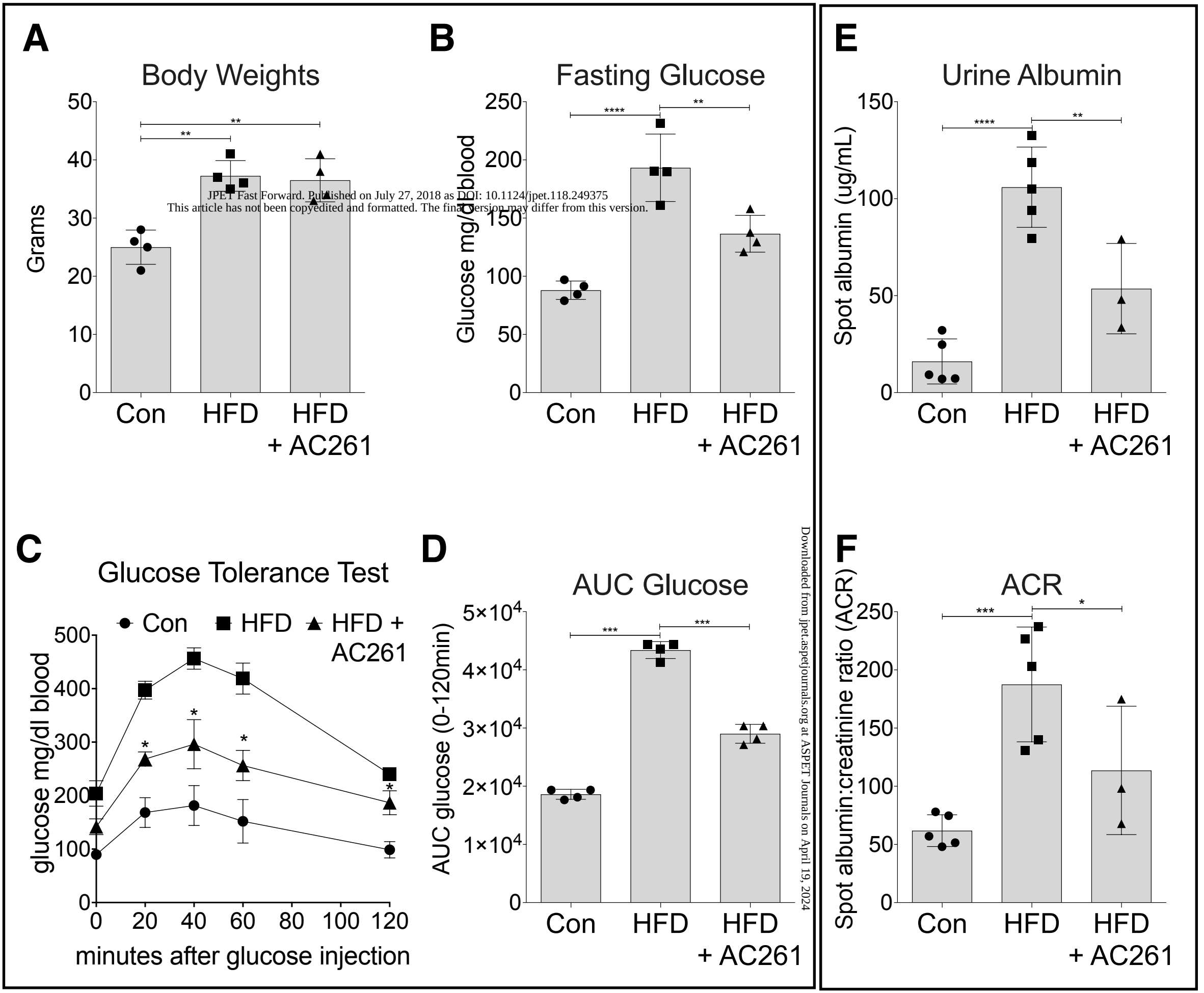

Figure 2

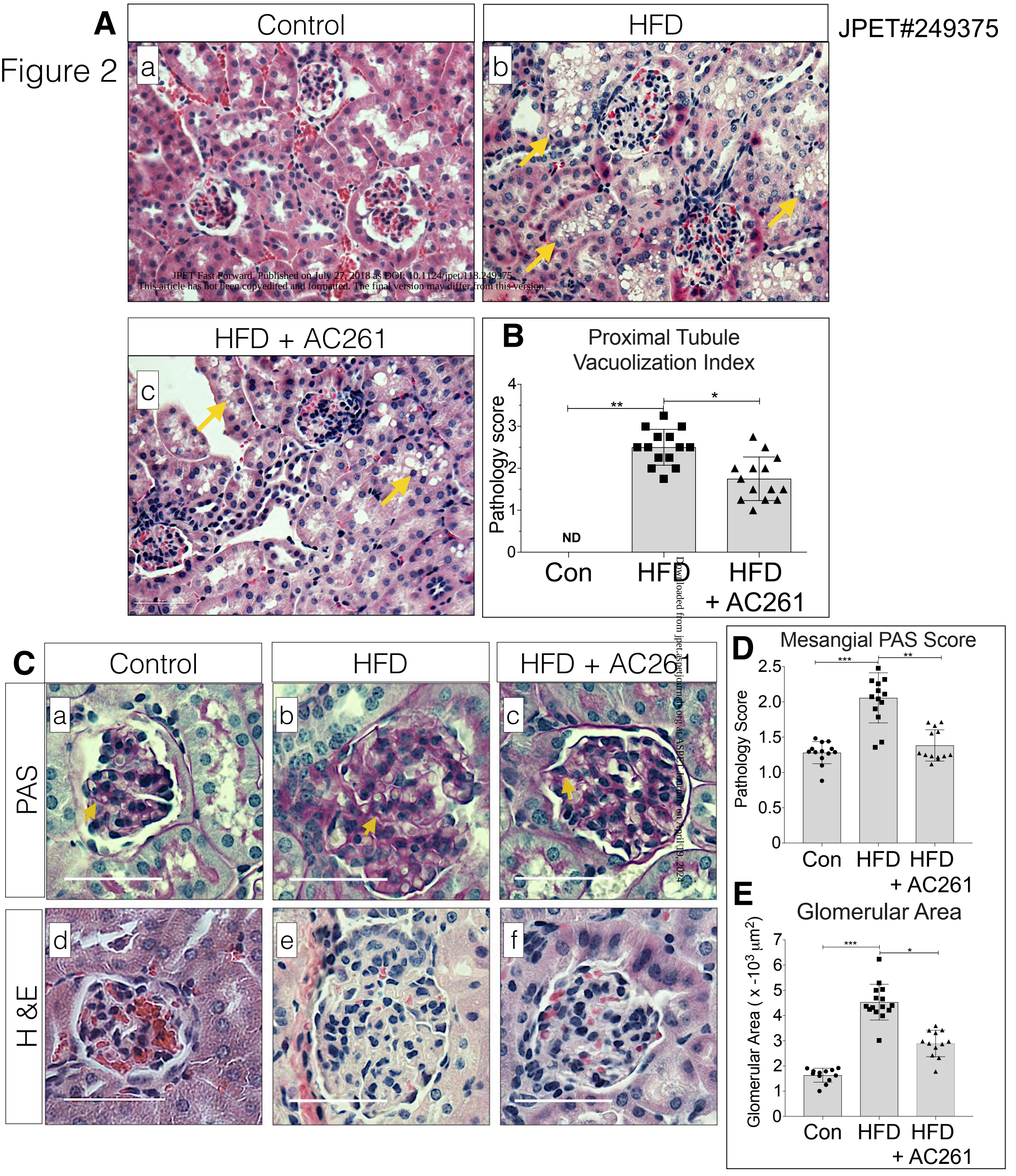

JPET Fast Forward. Published on July 27, 2018 as DOI: 10.1124/jpet.118.249375
This article has not been copyedited and formatted. The final version may differ from this version.

JPET#249375

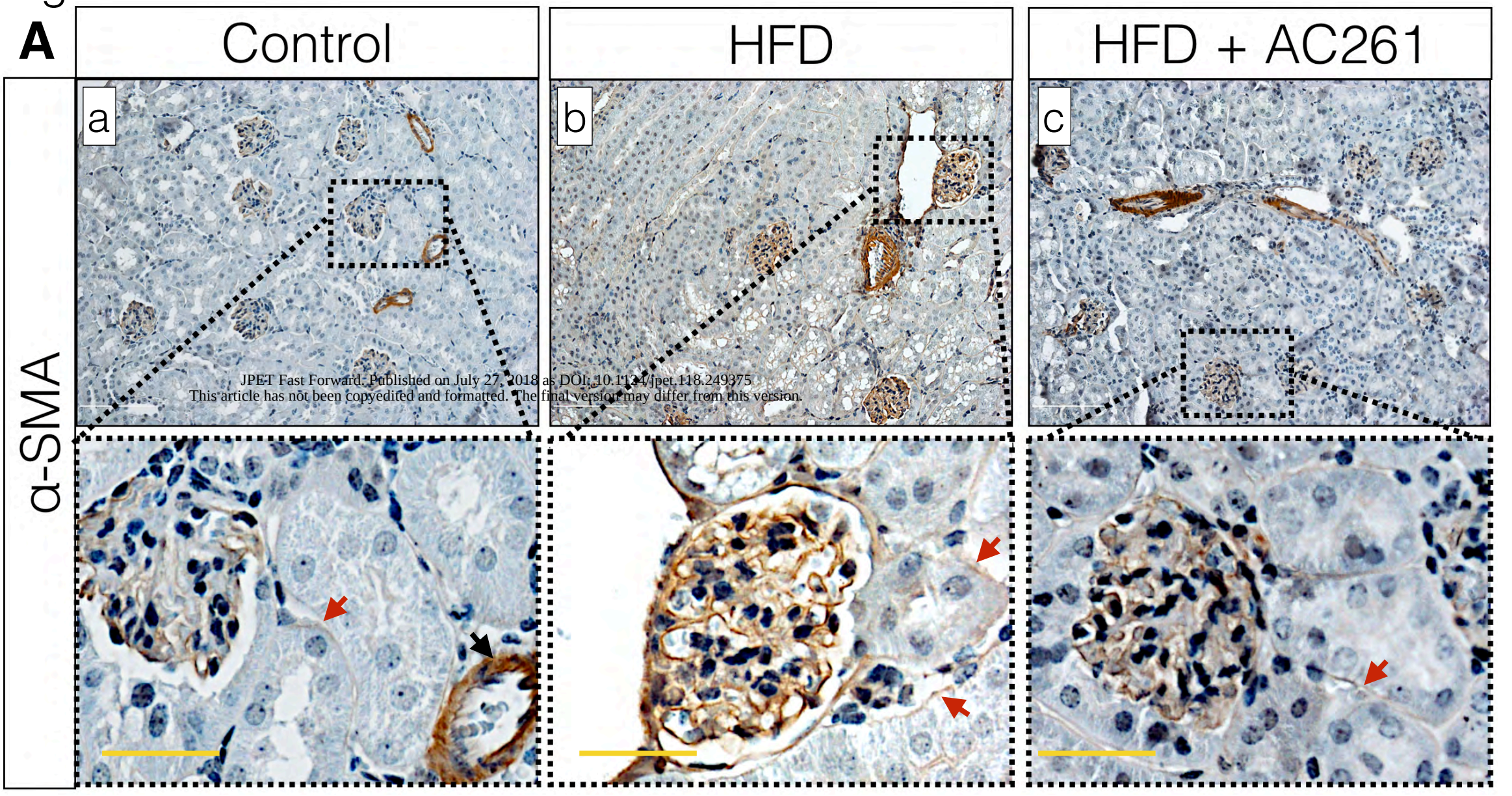

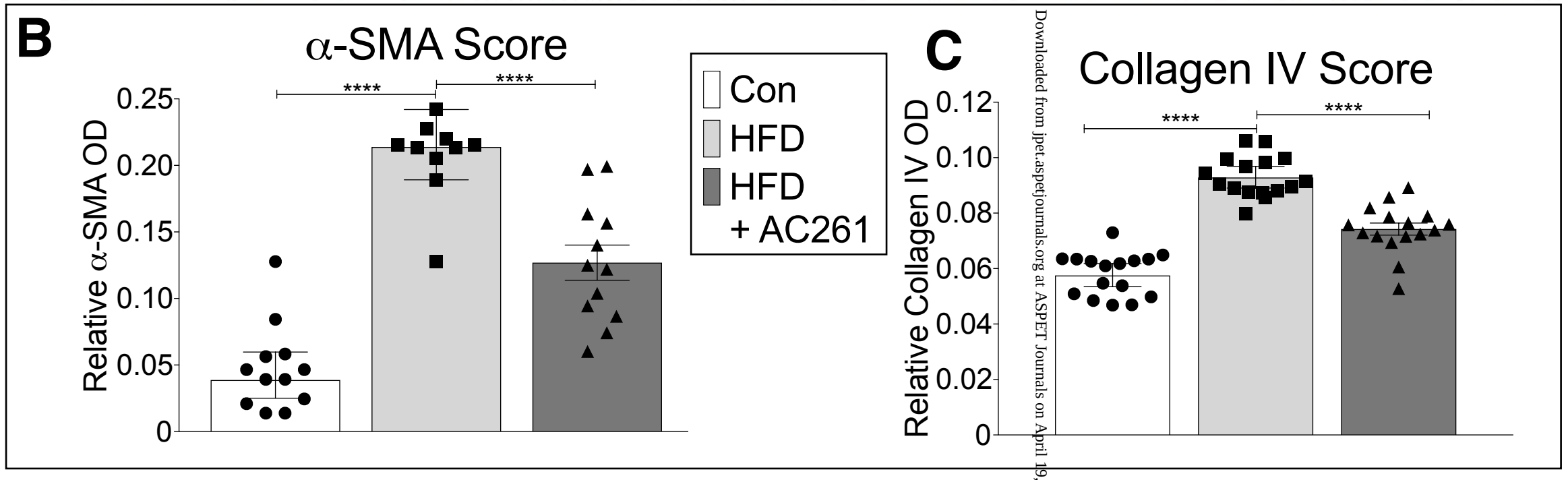

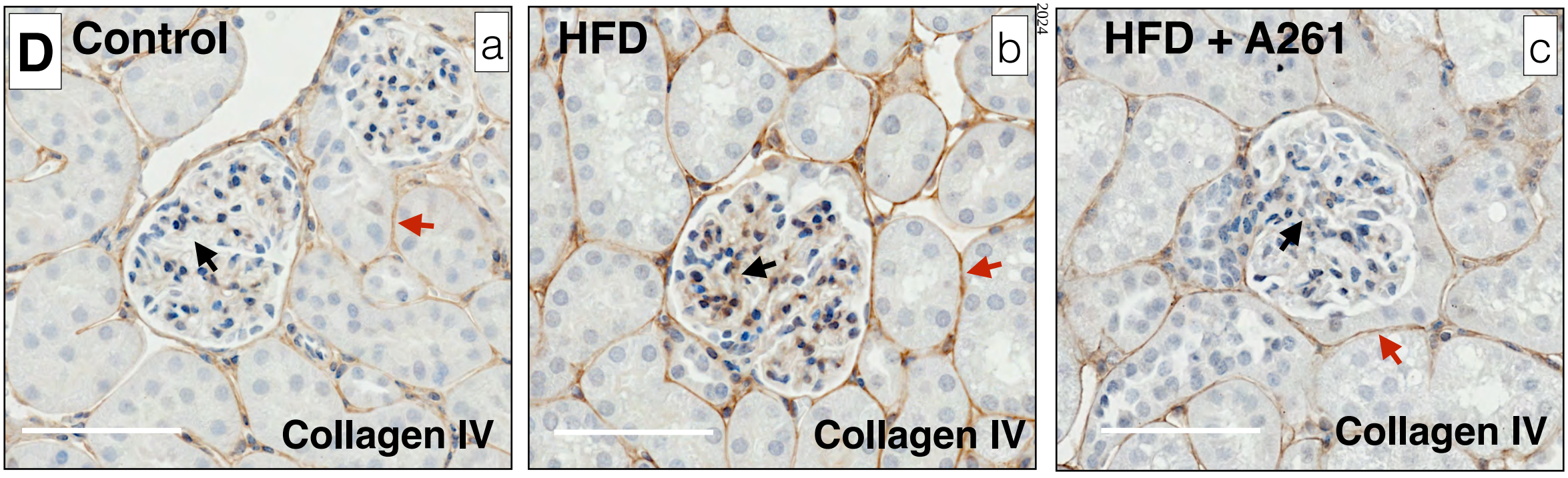

Figure 4

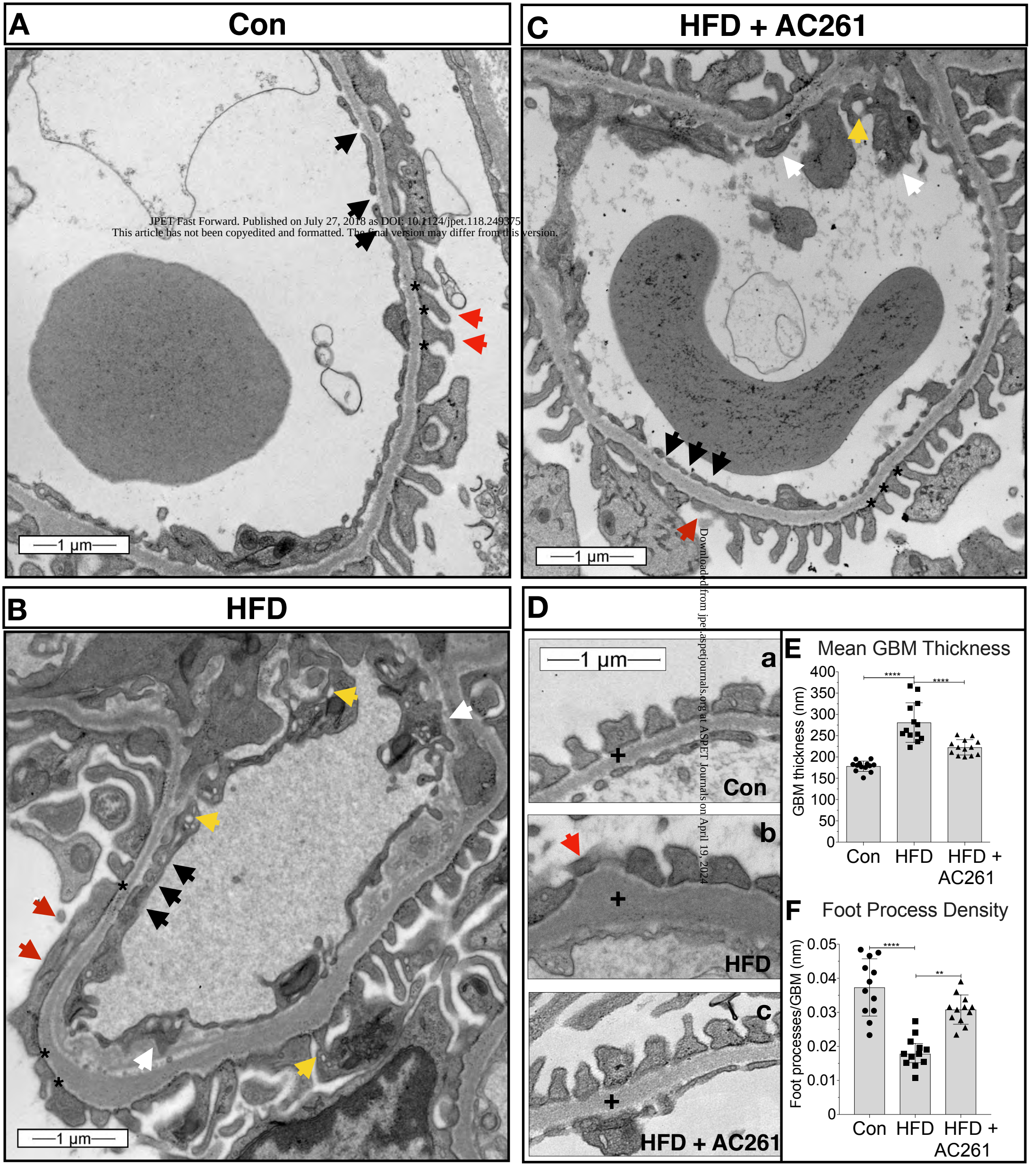

Figure 5

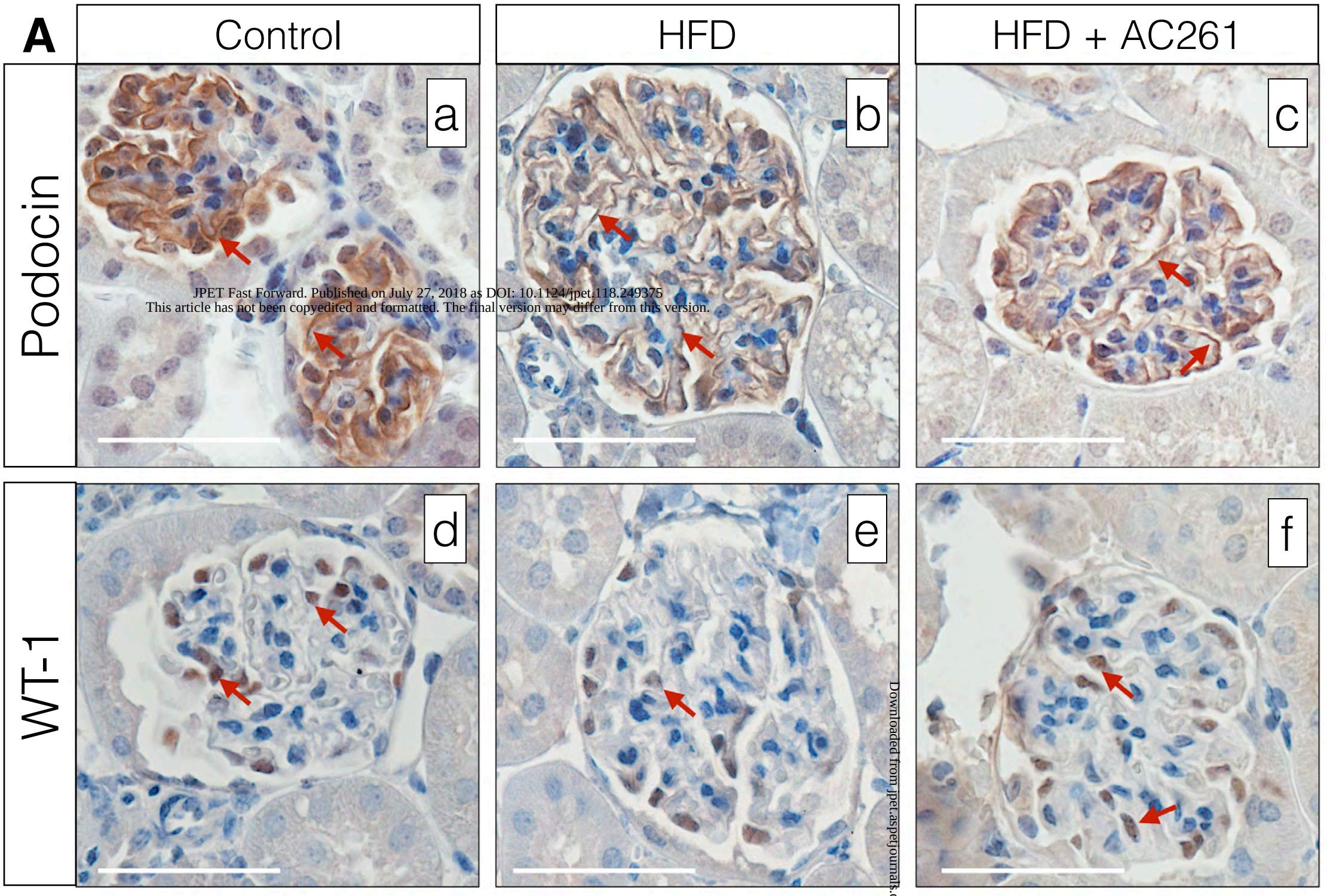

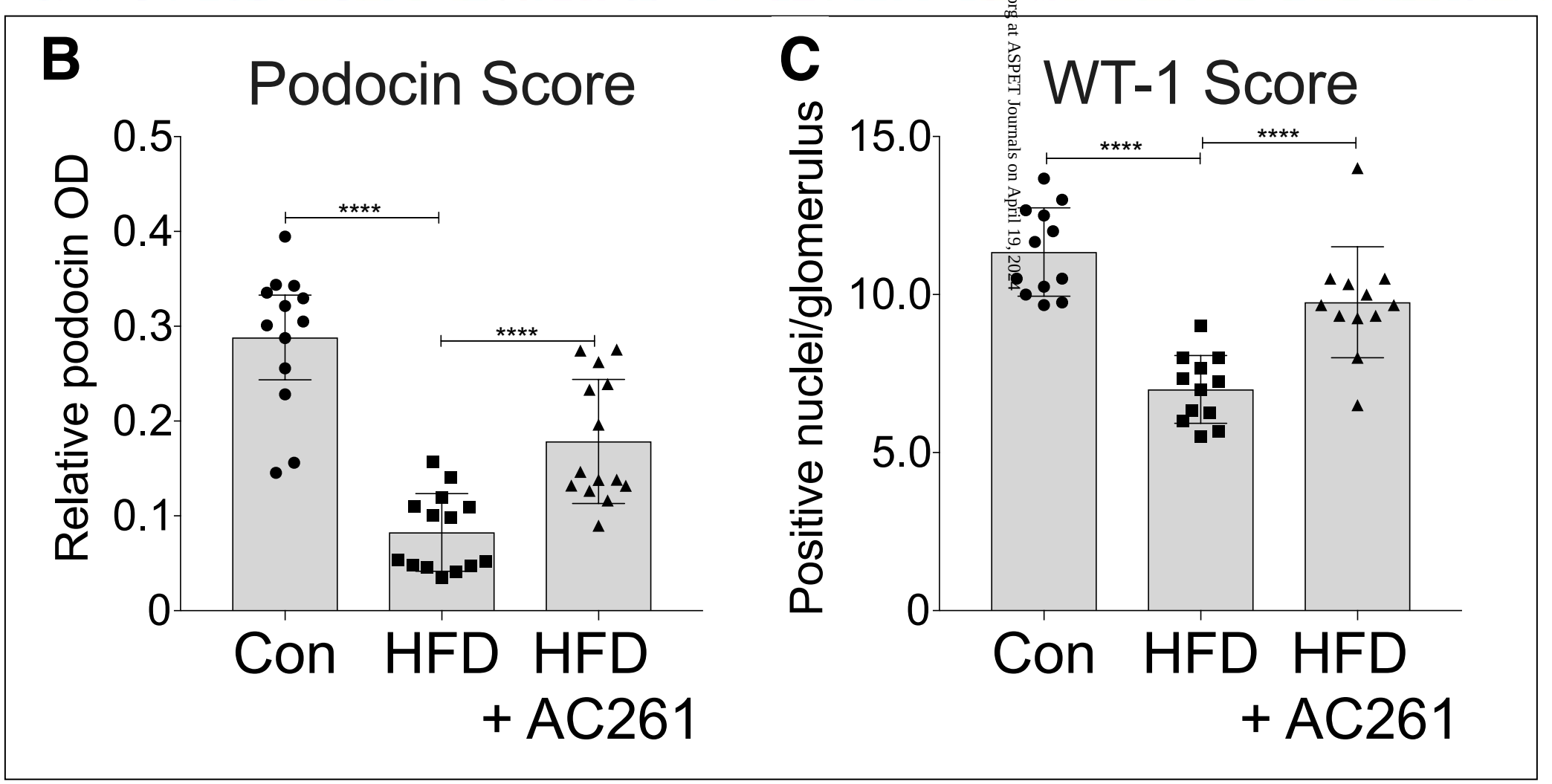

Figure 6

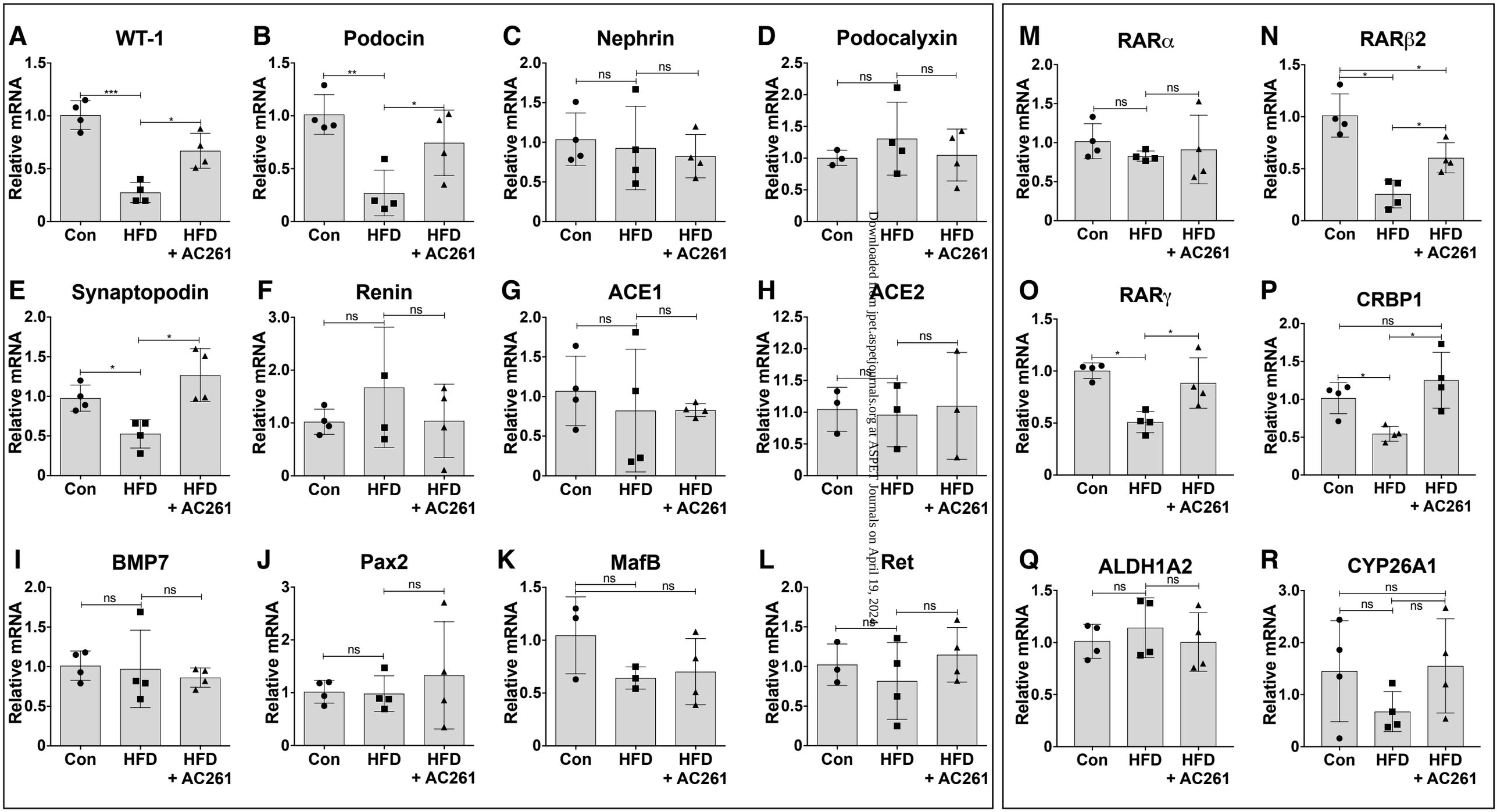

Figure 7